Off-grid Electrification Through Independent Solar Photovoltaic System

Master Thesis

By

BSc. Dexter Chintu

Study Program: Electrical Engineering, Power Engineering and Management

Branch of study: Electrical Power Engineering

Thesis Supervisor: Mgr. Ing. Ghaeth Fandi, Ph.D

Department Chair/College Dean: doc. Ing. Zdeněk Müller, Ph.D.

CZECH TECHNICAL UNIVERSITY IN PRAGUE

2023

MASTER'S THESIS ASSIGNMENT

I. Personal and study details

Student's name: **Chintu Dexter** Personal ID number: **472328**

Faculty / Institute: **Faculty of Electrical Engineering**

Department / Institute: **Department of Electrical Power Engineering**

Study program: **Electrical Engineering, Power Engineering and Management**

Specialisation: **Electrical Power Engineering**

II. Master's thesis details

Master's thesis title in English:

Off-grid Electrification Through Independent Solar Photovoltaic System

Master's thesis title in Czech:

Off-grid elektrifikace prostřednictvím nezávislého solárního fotovoltaického systému

Guidelines:

1) Analysis and review of the necessary methodology for isolated system
2) Efficiency calculations of independent solar photovoltaic system
3) Use system as a crisis case
4) Analysis of technical issues regarding stand-alone solar photovoltaic system

Bibliography / sources:

1) Fandi, G. et al. (2018) "Voltage Regulation and power loss minimization in radial distribution systems via reactive power injection and distributed generation unit placement," Energies, 11(6), p. 1399. Available at: https://doi.org/10.3390/en11061399.
2) Fandi, G. et al. (2018) "Design of an emergency energy system for a city assisted by renewable energy, Case study: Latakia, Syria," Energies, 11(11), p. 3138. Available at: https://doi.org/10.3390/en11113138.
3) Mertens, K. and Roth, G. (2014) Photovoltaics: Fundamentals, technology and Practice. Chichester, West Sussex: Wiley.
4) Ja ger Klaus-Dieter et al. (2016) Solar Energy: Fundamentals, Technology and Systems. Cambridge: UIT Cambridge.

Name and workplace of master's thesis supervisor:

Ing. Ghaeth Abdulhamid Fandi Department of Electrical Power Engineering FEE

Name and workplace of second master's thesis supervisor or consultant:

Date of master's thesis assignment: **09.02.2023** Deadline for master's thesis submission: _____

Assignment valid until: **22.09.2024**

Ing. Ghaeth Abdulhamid Fandi	doc. Ing. Zdeněk Müller, Ph.D.	prof. Mgr. Petr Páta, Ph.D.
Supervisor's signature	Head of department's signature	Dean's signature

III. Assignment receipt

The student acknowledges that the master's thesis is an individual work. The student must produce his thesis without the assistance of others, with the exception of provided consultations. Within the master's thesis, the author must state the names of consultants and include a list of references.

Date of assignment receipt	Student's signature

Declaration:

I hereby declare that this master's thesis is the product of my own independent work and that I have clearly stated all information sources used in the thesis according to Methodological Instruction No.1/2009 – "On maintaining ethical principles when working on a university final project, CTU in Prague".

Date Signature

Table of Contents

Contents

Acknowledgments

I would like to express my sincere gratitude to my supervisor, Mgr. Ing. Ghaeth Fandi, Ph.D., for his unwavering support, guidance, and encouragement throughout my thesis journey. His extensive expertise, profound insights, and essential guidance have significantly contributed to my enhanced comprehension of the topic and the refinement of my research abilities. His constant feedback, constructive criticism, and attention to detail have been instrumental in shaping the direction and focus of this research work. I`m truly grateful for his/her mentorship and inspiration, which have been a source of motivation and encouragement.

In addition, I would like to thank my family for their unwavering support, encouragement, and love throughout my academic journey. Their belief in me has been a driving force in my life, and I am grateful for their unwavering support and guidance.

Finally, I want to express my heartfelt appreciation to my life partner, Marie Kulkova. Her constant support, love, and understanding throughout the busy schedule of my studies and thesis journey. Her patience, understanding, and encouragement have been an essential source of inspiration, and I am forever grateful for her love and support.

List of Abbreviations

ESCO	Energy Service Companies
PV	Photovoltaic
DOD	Depth of Discharge
DG	Distributed Generation
MPPT	Maximum Power Point Tracking
PSO	Particle swarm optimization
PCC	Point of Common Coupling
REA	Rural Electrification Authority
SHS	Solar Home System
SPS	Solar Photovoltaic Systems
ZESCO	Zambia Electricity Supply Corporation Limited

Abstract

Access to electricity is a fundamental requirement for modern life and economic development. In numerous global regions, especially in rural zones, there exists a significant deficit in electrical accessibility, primarily attributed to the non-existence of grid infrastructure. Stand-alone solar photovoltaic systems (SPS) offer a viable solution to off-grid electrification by providing reliable and sustainable power for households, businesses, and communities.

This research paper aims to explore the design of stand-alone solar photovoltaic (PV) systems as a viable solution for off-grid electrification in a remote area in a small town in Zambia. The study employs a methodology to determine the required volume of the solar PV system to provide the needed power for operation and, most importantly, simulate this instance in MATLAB. The research presents the necessary technical considerations for assessing the load power demand per day and sizing the different components of the solar system, including the inverter, charge controller, storage batteries, PV panels, and other ancillary equipment such as cables.

Additionally, the study confirms that the stand-alone solar PV system is an effective and environmentally friendly way of supplying electrical energy, resulting in minimal carbon emissions and air pollution. The study focuses on Zambia, evaluating the current electrical situation and applying the study's findings to the region of the Eastern Province, Chalochasowa. The findings of this research indicate that independent solar PV systems may provide a dependable electricity supply for rural populations, contributing to sustainable growth and enhancing the living standards of the inhabitants.

Keywords: Solar PV, Off-grid Systems, Simulation, Simulink

1. Introduction

Access to reliable electricity is a fundamental prerequisite for social and economic development. However, more than 700 million people worldwide still lack access to electricity [1], particularly in rural and remote areas where the grid is either absent or unreliable.

A large portion of these communities lack sufficient, reasonably priced, and easily accessible energy sources due to their remote locations, which makes it challenging to expand centralized energy grids. Consequently, they are compelled to depend on conventional energy sources such as wood fuel, dung, and agricultural waste for cooking purposes, and kerosene for illumination. However, the use of these traditional fuels, particularly in arid and semi-arid regions, can result in environmental degradation through the excessive deforestation and clearing of woodlands, as well as detrimental health effects due to smoke inhalation leading to respiratory illnesses [2].

Off-grid electrification through independent solar PV systems offers many potential benefits beyond simply providing access to electricity. It can improve health outcomes by reducing reliance on kerosene lamps and other polluting sources of lighting and cooking, promote economic development by enabling small businesses and productive uses of electricity, and enhance education by providing reliable lighting for studying. Moreover, it has the potential to serve as a sustainable alternative to fossil fuels, reducing greenhouse gas emissions and combating climate change [3].

This dissertation offers an exhaustive examination of the methodology applied to an isolated system; thus, the technical challenges associated with stand-alone solar PV systems is the focus of this research. Through a comprehensive examination of issues like system stability, component compatibility, maintenance requirements, and potential grid interaction, the study aims to identify and address the key technical hurdles that hinder the widespread adoption of such systems, efficiency calculations of independent solar PV system-related to the system, analyse the technical issues regarding independent solar PV system and finally use the system as a crisis case.

Ultimately, this study aims to enrich the expanding pool of information regarding off-grid electrification, serving as a resource for decision-makers, practitioners, and academics by highlighting the technology's role in enhancing energy availability and supporting sustainable growth.

2. Problem Statement

2.1 Load Shedding in Zambia

Load shedding is a common occurrence in Zambia, especially during the dry season when there is a decrease in water levels at the country's major hydroelectric power plants. The country relies heavily on hydroelectric power, with about 85% of its electricity being generated from hydropower sources [5].

Load shedding in Zambia occurs when the electricity demand exceeds the supply, resulting in the power utility company, Zambia Electricity Supply Corporation (ZESCO), having to cut off power to certain areas for several hours at a time. This is done on a rotational basis, with different areas experiencing power outages at different times.

The impact of load shedding in Zambia is significant, with many households and businesses being affected. Some of the effects of load shedding include:

1. Disruption of business operations: Load shedding can lead to disruptions in business operations, especially those that require electricity to run, such as manufacturing and processing industries.
2. Loss of income: Load shedding can also lead to loss of income for businesses and individuals who are unable to operate during power outages.
3. Health risks: Load shedding can lead to health risks, especially for those who rely on electricity for medical devices, such as oxygen machines and refrigerators for storing medication.
4. Impact on education: Load shedding can also have an impact on education, with schools and universities having to close or reduce their operating hours during power outages.

A study by Samboko et al. [6] investigated the link between load shedding and charcoal use in Zambia. The study found that load shedding increased the demand for charcoal as a substitute for electricity for cooking and heating purposes. This increased charcoal production, and consumption had negative effects on forest resources and greenhouse gas emissions. The study estimated that load shedding resulted in an additional loss of 127,000 hectares of forest land and an additional emission of 4.5 million tons of carbon dioxide equivalent per year. Therefore, load shedding is a serious challenge for Zambia that requires urgent and sustainable solutions.

2.2 Difficulties in scaling up renewable energy production.

Zambia has been facing a severe electricity supply crisis despite having over 2,500 MW of installed capacity. The issue is largely attributed to droughts that have affected the hydro-based power system. In response, the government has made efforts to address the problem by aiming to procure 600 MW of solar PV capacity through the World Bank's Scaling Solar program. The program is designed to facilitate the development of privately owned solar PV projects in sub-Saharan Africa, with a focus on completing projects [4].

The current situation of renewable energy in Zambia is promising but also challenging. Zambia faces several barriers to scaling up renewable energy deployment, such as:

1. The integration of variable renewable sources into the grid is limited by inadequate transmission and distribution infrastructure.

2. The high cost of renewable energy technologies and equipment makes them unaffordable for many consumers and investors.

3. The lack of clear and consistent policies and regulations creates uncertainty and confusion for renewable energy stakeholders.

4. The absence of adequate financial access and credit provisions impedes the progress of renewable energy initiatives and enterprises.

5. The lack of awareness and information on the benefits and opportunities of renewable energy among the public and private sectors [35].

3 Energy in Zambia

Zambia is a landlocked country situated in the south-central region of Africa, with a total area of 752,618 square kilometers (slightly larger than France). It is positioned on an elevated plateau, with its altitude ranging from 900 to 1,500 meters above sea level [48]. Zambia is bordered by eight countries: Angola to the west, Namibia, Botswana, Zimbabwe, and Mozambique to the south, the Democratic Republic of the Congo and Tanzania to the north, and Malawi to the east. Zambia's capital and largest city is Lusaka, located in the south-central part of the country. Zambia's population was estimated at 18.9 million in 2020 [34].

Figure 1: Location of Zambia in Africa with respect to the Tropical of Cancer, Capricorn, and

In 2018, the Republic of Zambia boasted an installed electricity generation capacity of approximately 3,000 megawatts (MW), predominantly harnessed from hydroelectric sources. The peak demand for electricity during that year was observed to be approximately 650 MW lower than the installed capacity. Notwithstanding, post-2018, there has been a discernible decline in available capacity, culminating in a significant supply shortfall exceeding 810 MW by 2020. The access to electrical power exhibits considerable disparity, being markedly deficient in rural areas compared to urban locales, with electrification rates as low as below 5% in rural regions, in stark contrast to approximately 80% in urban settings [43].

Despite the glaring lack of electricity access for over 2 million households and the supply deficit, the per capita electricity consumption in Zambia is nearly double the average observed across the sub-Saharan African region. This consumption is predominantly driven by industrial sectors, which are responsible for more than half of the total electricity utilization.

Projected estimations indicate a substantial escalation in peak electricity demand in Zambia, anticipated to reach approximately 4,247 megawatts (MW) by the year 2025, a significant increase from the 2,194 MW recorded in 2018. Concurrently, the national objective is to achieve an electrification rate encompassing 66% of the population by the year 2030 while also aspiring to augment the installed electricity generation capacity to an estimated 6,000 MW, effectively doubling the capacity figures of 2018. Despite the liberalization of the country's energy sector, which has permitted private enterprise participation for over two decades, Independent Power Producers (IPPs) have struggled to establish a substantial foothold or widespread adoption within the sector.

The IPP market in Zambia is predominantly dominated by a limited number of companies that specialize in generating electricity from major hydroelectric and thermal sources, subsequently distributing this energy to the national grid. In contrast, there are a number of smaller-scale enterprises focusing on solar and hydroelectric power generation, primarily targeting rural areas with their services. Notably, two expansive solar energy projects are slated to commence construction in 2020, following the execution of a memorandum of understanding with the Zambian government. These projects collectively contribute an additional 200 MW to the national electricity grid, with a 135 MW installation planned for Northern Zambia and a 65 MW installation in the Copperbelt region of the country [43].

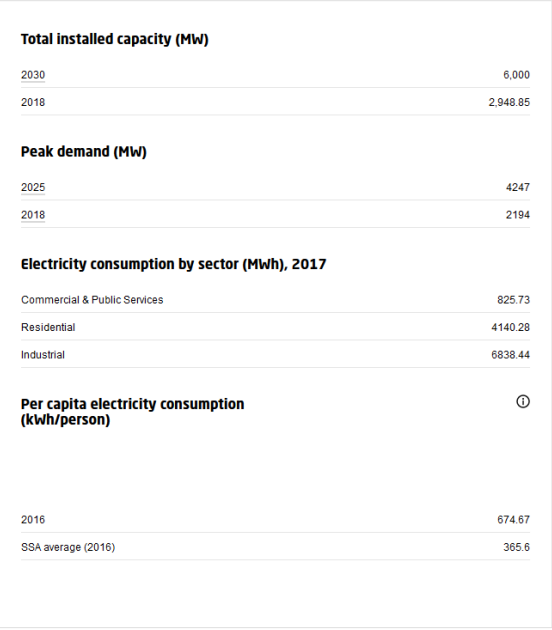

Figure 1: Total installed generation capacity by 2018 and predicted capacity in 2030 [43]

3.1 Renewable energy in Zambia

Renewable energy stands as a key focus in Zambia's efforts to broaden its energy mix and decrease reliance on traditional energy sources, including hydropower and fossil fuels. Currently, hydropower is the dominant source of electricity in Zambia, accounting for over 90% of the country's total installed capacity [4]. Nonetheless, the nation possesses considerable potential for additional renewable energy sources, including solar, wind, and geothermal power.
Solar energy is a particularly promising area for Zambia, as the country has abundant sunshine throughout the year. In 2019, the government launched the Scaling Solar program, which aims to facilitate the development of up to 54MW of solar power capacity in the country. The program provides a comprehensive package of support to developers, including assistance with project development, financing, and procurement [5].

By 2021, Zambia's renewable energy capacity amounted to approximately 2.7 gigawatts. In 2012, the installed capacity was around 1.9 gigawatts, and since then, there has been a consistent upward trend. Currently, renewable energy accounts for 83.7 percent of the country's electricity capacity [12].

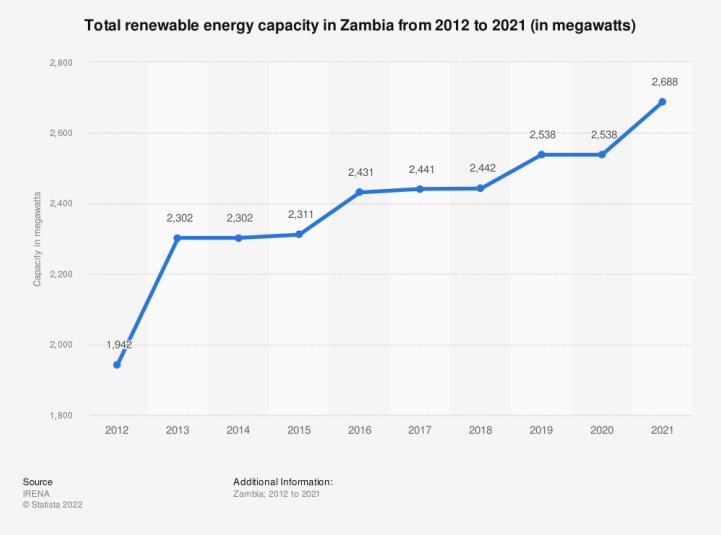

Figure 1.1: Total renewable energy capacity in Zambia from 2012 to 2021

3.2 Solar Photovoltaic in Zambia

Solar PV power is a renewable energy source that provides dependable local energy production with minimal greenhouse gas emissions. The sun's energy can be harnessed using different technologies to produce useful forms of energy, including heat and electricity. The practicality and viability of these technologies depend on the amount of solar energy available in a particular area [13].

The Earth's round shape and its orbit around the sun cause the sun's rays to strike the Earth at various angles, ranging from just above the horizon to directly overhead, depending on the location.

The Equator, Tropic of Cancer (23.50 degrees north of the Equator), and Tropic of Capricorn (23.50 degrees south of the Equator) are important latitude lines that help determine the sun's position throughout the year. For instance, on June 21st, the sun aligns directly over the Tropic of Cancer, leading to summer conditions in the northern hemisphere and winter in the southern hemisphere. In contrast, on December 21st, the sun is positioned directly above the Tropic of Capricorn, which brings about winter in the northern hemisphere and summer in the southern hemisphere. Conversely, on December 21, the sun is directly above the Tropic of Capricorn, resulting in winter in the northern hemisphere and summer in the southern hemisphere [48]. The regions bounded by the Tropic of Cancer and the Tropic of Capricorn experience a tropical climate with two distinct seasons: a rainy season and a dry season. Meanwhile, regions located north of the Tropic of Cancer and south of the Tropic of Capricorn experience four seasons a year: winter, autumn, spring, and summer. Figure 2 illustrates the Tropics of Cancer and Capricorn marked locations and where the rays of the noon sun are perpendicular to the ground at the solstices [49].

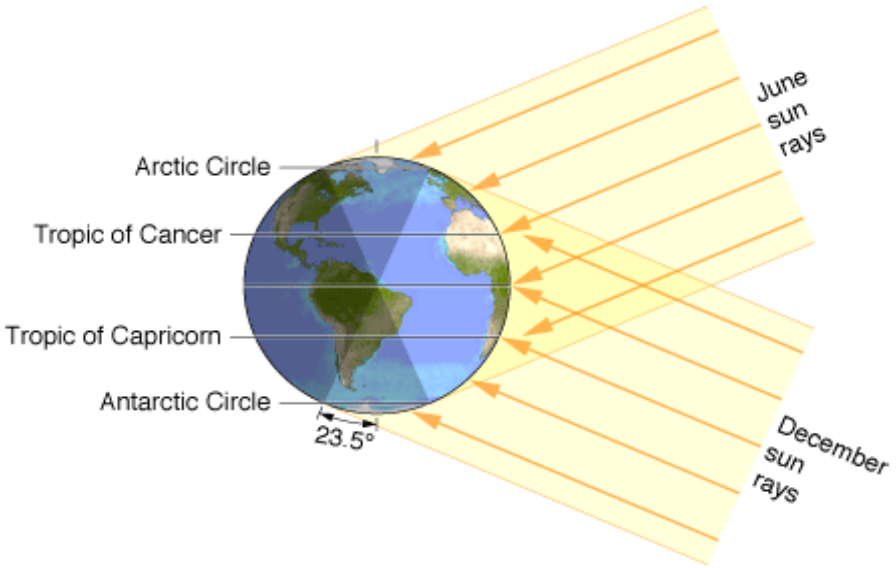

Figure 2: The Arctic and Antarctic Circles represent the northernmost and southernmost points, respectively, at which the sun's rays reach during the solstices. On the other hand, the Tropics of Cancer and Capricorn indicate the locations where the sun's rays are perpendicular to the ground at noon during the solstices. [14]

When the sun's rays are perpendicular to the Earth's surface, the Earth receives the highest amount of energy. As the angle of the sun's rays increases, the distance they travel through the atmosphere also increases. This causes the sunlight to spread out and become more scattered [15].

Zambia's location and the amount of solar radiation it receives make it highly conducive for solar power generation. Research and analysis done in the past by Zambia's Meteorological Department show that it has a sizable capacity for solar energy production and thermal usage. With an average daily sunshine duration of 7 to 8 hours and a consistently high monthly average solar radiation rate of 5.5kWh/m2 per day throughout the year, Zambia is located between latitudes of 8 to 18 degrees south of the equator and longitudes of 22 to 34 degrees east of the prime meridian [16, 36].
A number of PV projects have been started by the Zambian government through the Rural Electrification Authority (REA) with the goal of increasing access to energy. One such project is a

60kW solar off-grid installation in Mpanta, Samfya district of Luapula Province, which currently powers about 50 households. Furthermore, through the Energy Service Companies (ESCO) pilot project, REA has installed 400 solar home systems in addition to nearly 250 solar PV systems in schools and traditional authority buildings. However, a thorough analysis of the distribution and capacity for solar energy generation across the nation has not yet been conducted [36]. Although Zambia has one of the highest levels of annual solar radiation in the world, the country encounters obstacles and difficulties in distributing and utilizing this energy potential as an alternative for generating electricity. The majority of the installed systems are owned by individuals and are considered "off-grid," consisting of a combination of a solar array, inverter, and battery storage [17].

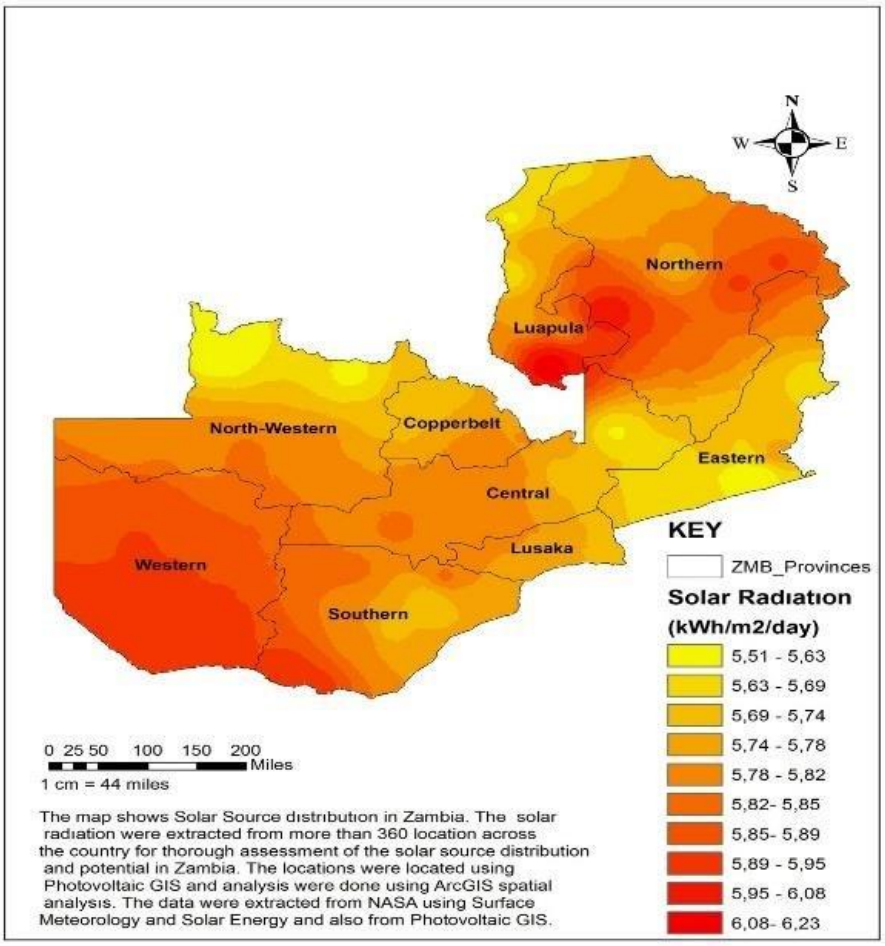

Figure 2.2: The Spatial Variation and Potential of Solar Energy in Zambia's Regions in the figure above illustrate that most Zambia's regions receive radiations higher than the national annual average radiations of 5.78kWh/m with western, southern, northern, and part of Luapula regions exhibiting the most favourable annual average radiation above 5.80kWh/m. It also indicates that the annual solar radiation in the country varies from 5.51 to 6.23kWh/m. [37]

4. Solar PV Categorization

Solar PV systems represent a pivotal advancement in renewable energy technology, offering a sustainable and increasingly cost-effective means of electricity generation by harnessing the natural energy from the sun; these systems convert solar radiation into electrical energy through the photovoltaic effect, a process whereby light energy induces the generation of voltage and current in a material [50]. The core component of these systems is the solar panel, an assembly of PV cells typically made from silicon, which exhibits semiconducting properties essential for this conversion process.

The efficiency and viability of solar PV systems have seen remarkable improvements, which are attributable to ongoing research and technological advancements. These systems are highly scalable, ranging from small rooftop installations for individual household use to large, utility-scale solar farms that contribute significantly to the electrical grid. The environmental benefits of Solar PV systems are substantial, offering a reduction in greenhouse gas emissions and a decrease in dependency on fossil fuels. As a cornerstone of renewable energy strategies, Solar PV systems are integral to addressing global challenges of climate change and energy security, making their study and development a key focus in the field of sustainable energy technology.

Solar PV systems in Zambia come in a variety of sizes, ranging from small applications like solar lanterns and mobile phone chargers to solar home systems installed in private households. Despite being categorized as a distinct type of technology, solar PV energy differs significantly in terms of technological features, size, capital requirements, competing technologies, and target markets [18]. When setting up a PV system, it's essential to use maximum power point tracking (MPPT) for the solar array. This technique not only boosts the power output of the solar PV system to the load, but it also increases its lifespan. Rooftop PV-generated electricity can be utilized as a stand-alone system or linked to the 220 V, 50 Hz power grid to supplement its power [19].

4.1 Grid-Tied Solar PV Systems

The installation of grid-connected solar PV systems is fairly straightforward, requiring only a few solar panels (modules) connected to an inverter, which is then linked to the building's electrical distribution via switchgear and kWh metering. Figure 3 shows a simplified grid connected PV system. However, despite its apparent simplicity, designing a system that is both safe and cost-effective can be a challenging and sometimes poorly executed task. In addition, solar power systems can be complemented with solar water heating, solar refrigeration, and solar water pumping systems.

Prior to installing solar systems, a thorough analysis of consumption requirements, solar irradiation, pitch, orientation, and temperature is typically conducted to enable solar installers to choose solar modules with the appropriate specifications. The installation can be completed on the client's rooftop or ground mount [18].

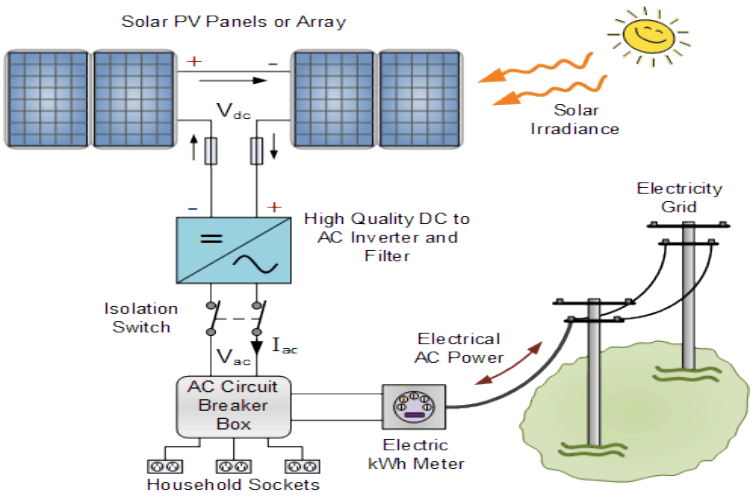

Figure 3: Simplified Grid-Connected PV System [20]

The grid-connected system fulfils two critical functions: firstly, it engages in the pursuit of optimal power extraction from the solar panels, facilitated through an appropriate MPPT converter. Secondly, it ensures that the voltage at the Point of Common Coupling (PCC) is sinusoidal and commensurate with the grid voltage. Additionally, various international societies establish specific norms that guide power utilities globally. The IEEE 1547 standard delineates stringent limitations on the maximum permissible current injected into the grid, setting it at a notably low threshold (less than 0.5% of the rated current). Enhancements in this parameter can be achieved through galvanic isolation between the PV system and the grid. However, this poses a significant challenge in the context of transformerless inverters, necessitating precise calibration of the DC current value. The EN 50106 standard specifically addresses permissible voltage deviations at the PCC. Uniquely, the German VDE-0126 standard focuses on the range of leakage current in transformerless systems. This standard also specifies the required disconnection interval for inverters from the grid, triggered when the leakage current exceeds 30 mA [44].

4.2 Stand-alone Solar PV System

A standalone solar power system presents an optimal choice for individuals aiming to diminish their carbon footprint and enhance energy efficiency, serving as a viable alternative to conventional power sources. The system comprises various critical elements, including a PV panel array for solar energy capture, a charge controller to manage battery charging and discharging, and a battery bank for power storage (see Figure 4). One critical feature of the stand-alone solar power system is the charge controller, which prevents overcharging or undercharging of the battery. This function helps prolong the battery's lifespan, reduces maintenance costs, and ensures optimal performance.

Another key component of the system is the inverter, which converts DC power to AC power, making it suitable for operating AC appliances [21]. This optional component allows for greater flexibility and convenience when using the solar power system to power household appliances and electronics. Stand-alone solar systems are preferred because of their simplicity, ease of use, and hassle-free nature. The basic operating procedure of a stand-alone solar system involves the conversion of sunlight into electricity using angled PV panels, which varies depending on the location. The charge controller regulates the electricity generated by the solar system, and any surplus power can be stored in batteries for backup use when sunlight is unavailable.

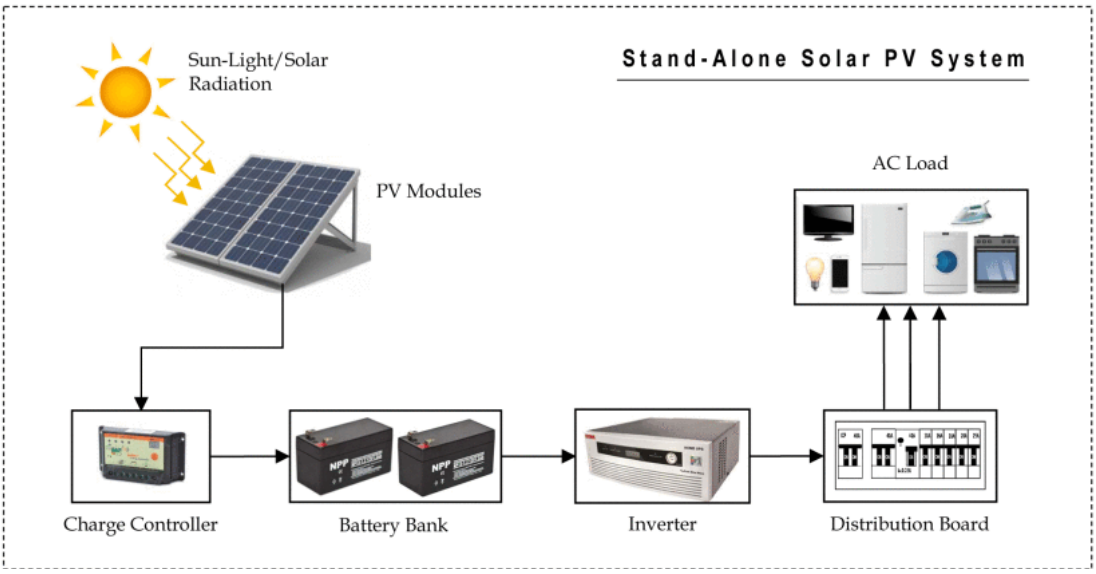

Figure 4: Configuration of stand-alone solar PV energy system [21].

The stand-alone solar PV system has two main pathways;

a) **Systems designed for single households** typically serve as an initial step in technological advancement. This classification encompasses devices like solar lanterns and solar home systems. While their capabilities are confined to a restricted range of functions, their compact and modular nature renders them financially accessible to consumers at the lower end of the economic spectrum.

b) **Centralized local systems**, known as collective systems, supply power to a cluster of users comprising both residential and commercial entities. This group encompasses mini and micro grids operating in either alternating current or direct current modes. These smaller-scale utilities facilitate a broader spectrum of activities, including energy for productive purposes. Recently, there has been a heightened focus on these systems as supplementary to grid-based electrification. They are considered a viable option for enhancing electrification rates in the rural regions of developing nations.

While both individual devices and collective systems have experienced growth recently, the former holds a larger share of the market. Solar lanterns, known for their portability, ease of use, inherent safety, cleanliness, and affordability, are gaining popularity. Some modern versions even include additional features like mobile charging and radios, enhancing their utility. However, solar home systems (SHS) are predominant in off-grid solar PV-based electrification. They provide a broader range of services than solar lanterns due to their higher power capacity, enabling households to use a variety of appliances such as lights, fans, televisions, and radios. Initially, SHS was large (50–150 Wp) and only affordable for wealthier households, limiting their market size.

Over time, smaller systems have been introduced to the market, making them more accessible to lower-income households. Systems of 10 or 20 Wp are now widely available in many countries. The advent of LED lighting has further facilitated this miniaturization, as it significantly lowers power requirements. Additionally, the development of efficient DC appliances has expanded the range of services available to rural households. Portable solar kits have become increasingly popular due to the advancements that have been made in the technology. These kits, which require neither installation nor extensive maintenance and are more cost-effective than fixed SHS, are becoming both affordable and well-received products [44].

5. Basic Calculation Relationships and Assumptions

5.1 The Solar Cell

The solar PV cells used in grid-connected systems worldwide can be classified into two categories: crystalline (Figure 6) and thin film (Figure 7). Crystalline cells are the predominant type, comprising more than 90% of the PV systems in use, which includes those on solar farms and building rooftops [23, 24]. Although crystalline cells are pricier, they usually have higher efficiency rates and longer warranties for performance. To manufacture silicon cells, a thin top layer is doped with Boron, while a thicker lower layer is doped with Phosphorus. The doped layers generate a "depletion zone" in between them, creating an electric field [24]. In PV modelling, solar energy is directly transformed into electricity through the use of a PV cell. The panel used in PV modelling operates based on the photoelectric effect. To model a PV system, an inverted diode is connected in parallel with a current source, as well as a series and parallel resistance [25].

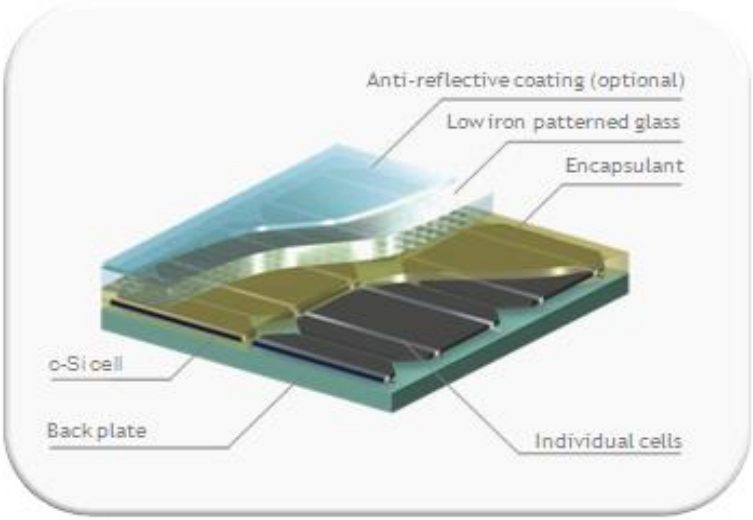

Figure 5: Crystalline solar cell [26].

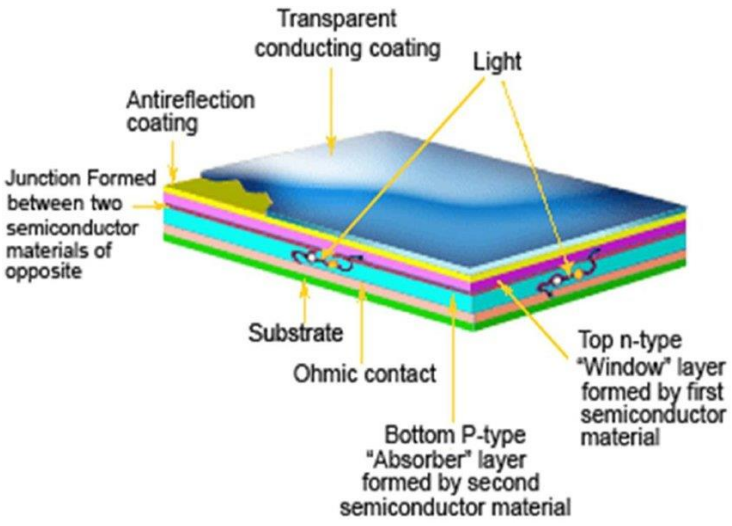

Figure 6: Thin film solar cell

5.1.1 Single Diode Model

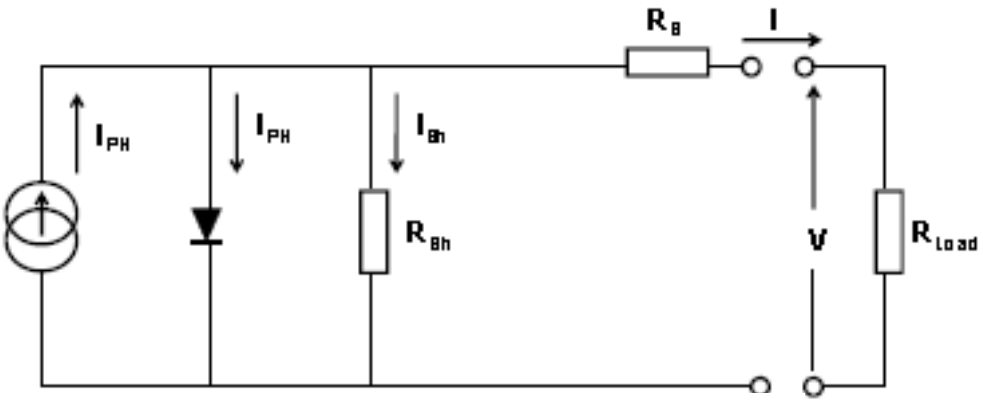

Figure 7: Solar cell modelling using one diode. [29]

A single diode mode refers to the operating state of a diode where it is forward-biased, allowing current to flow through it in one direction while blocking current flow in the opposite direction [51]. In this mode, the diode acts like a one-way valve for electric current. When a diode is forward-biased, it means that the voltage across the diode is such that the positive end of the voltage source is connected to the diode's anode (positive terminal), and the negative end is connected to the diode's cathode (negative terminal). This causes the diode to conduct electricity and allow current to flow through it. On the other hand, when the voltage polarity is reversed, the negative end of the voltage source is connected to the diode's anode, and the positive end is connected to the diode's cathode, the diode becomes reverse-biased and blocks current flow [28].

The behaviour of a diode in the forward-biased mode is governed by the diode's current-voltage characteristic, which is nonlinear and can be approximated as an exponential function. The current through the diode increases exponentially with increasing forward voltage while the voltage drop across the diode remains roughly constant.
The single-diode mode is used in a wide range of electronic circuits, including rectifiers, voltage regulators, and signal detectors. In rectifiers, diodes are used to convert AC voltage into DC voltage by allowing current to flow only in one direction. In voltage regulators, diodes are used to maintain a constant voltage by dropping a fixed amount of voltage across the diode. In signal detectors, diodes are used to demodulate amplitude-modulated radio signals by allowing only the positive half of the signal waveform to pass through the diode [28].

The single diode can be represented by the parameters I_{rs}, T, I_{sc}, I_{ph}, I_r, and k_i, where I_{rs} stands for the reverse saturation current of the module, T is the temperature at which it operates, I_{sc} is the short circuit current, I_{ph} represents the photocurrent, I_r is the solar irradiation, and k_i represents the short circuit of the cell under certain temperature and radiation conditions.

$$I_{ph} = (I_{sc} + k_i(T - 298))\frac{I_r}{1000} \quad (1.1)$$

$$I_{rs} = \frac{I_{sc}}{\exp\left(\frac{qV_{oc}}{N_s KnT}\right) - 1} \quad (1.2)$$

Where q is electron charge (1.6 × 10-19C),

The solar module's open circuit voltage, denoted as V_{oc}, is measured at 21.24 volts, with N_s indicating the number of cells linked in series. The Boltzmann constant, k, is equal to 1.3805×10-23 J/K, and the Ideality factor is represented by n and has a value of (1.6).

The temperature is subject to changes due to variations in altitude and seasonal conditions, such as the rainy or dry season. The saturation current of the module, I_0, is affected by fluctuations in the temperature of the cell. This is given by:

$$I_0 = I_{rs}\left(\frac{T}{T_n}\right)^3 exp^{\frac{q \times E_{go}}{nk}}\left(\frac{1}{T} - \frac{1}{T_n}\right) \quad (1.3)$$

Here, T_n: nominal temperature is 298.15 K, E_{go}: band gap energy of the semiconductor is 1.1 eV.

The electrical current generated by the PV module is expressed as:

$$I = N_p I_{ph} - N_p I_o \left(\exp^{\frac{\frac{V}{N_s} + I\frac{R_s}{N_p}}{NV_t}} - 1 \right) - I_{sh} \quad (1.4)$$

The values N_p, R_s, R_{sh}, and V_t correspond to the number of PV modules connected in parallel, the series resistance, the shunt resistance, and the diode thermal voltage, respectively.

$$V_t = \frac{kT}{q} \quad (1.5)$$

$$I_{sh} = \frac{\left(V\frac{N_p}{N_s}\right) + IR_s}{R_{sh}} \quad (1.6)$$

5.1.2 The Two Diode Model

In the single-diode equation, the ideality factor, represented by "n," is dependent on the voltage applied to the device. At higher voltages, recombination is mainly influenced by the bulk and surface regions, resulting in an ideality factor that is approximately equal to one. In contrast, when operating

at reduced voltages, the junction primarily dictates the recombination process, resulting in the ideality factor escalating to a value of two.

It should be emphasized that the ideality factor is not a static value; rather, it is a dynamic parameter subject to variation in accordance with the diode's operating conditions. The accurate determination of the ideality factor is essential for the proper modelling and analysis of PV systems.

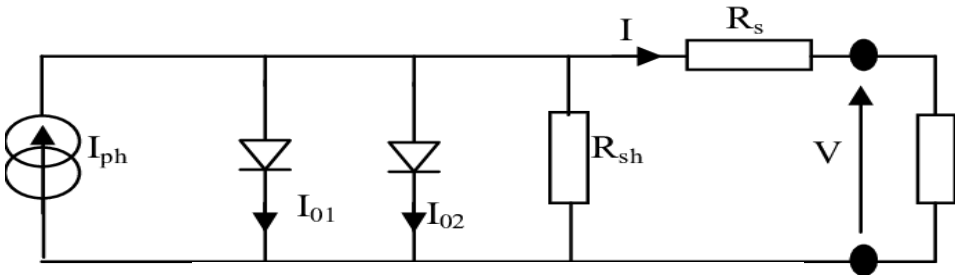

Figure 8: Equivalent circuit of a two-diode model solar cell [30]

A common way to represent the main characteristics of PV devices is the two-diode model. This model has an electrical equivalent circuit, which is shown in Figure 8. The circuit configuration includes a light-sensitive current source, two diodes connected in parallel, a parallel resistor, and a series resistor. The terminal voltage and current of the PV cell can be mathematically described by the following equation:

$$I = \mathrm{I_{pv}} - \mathrm{I_{01}} - \mathrm{I_{02}} - \frac{\mathrm{V} + \mathrm{R_s} l}{\mathrm{R_{sh}}} \tag{1.7}$$

This can be expressed using Shockley's diode equation as follows:

$$I = \mathrm{I_{ph}} - \mathrm{I_{01}}\left[\exp\left(\frac{\mathrm{q(V} + \mathrm{R_s} l}{n_1 kT}\right) - 1\right] - \mathrm{I_{02}}\left[\exp\left(\frac{\mathrm{q(V} + \mathrm{R_s} l}{n_2 kT}\right) - 1\right] - \frac{\mathrm{V} + \mathrm{R_s} l}{\mathrm{R_{sh}}} \tag{1.8}$$

The thermal voltage can be expressed as a simplified version of equation (1.8), which includes I_{ph} as the photocurrent, I_{01} and I_{02} as the saturation currents of the diodes, n_1 and n_2 as their ideality factors, q as the electron charge, k as the Boltzmann constant, T represents the temperature of the p-n junction measured in Kelvin, while R_s and R_{sh} denote the series and shunt resistances, respectively.

$$V_t = \frac{\mathrm{kT}}{\mathrm{q}} \tag{1.8.1}$$

To increase the power of PV devices, they often have many PV cells that are connected in different ways. Some cells are connected in a series to raise the voltage, and some cells are connected in parallel to raise the current. This can be included in the model with this equation.

$$I = \mathrm{I_{ph}} - \mathrm{I_{01}}\left[\exp\left(\frac{\mathrm{V} + \mathrm{R_s}l}{n_1 N_s V_t}\right) - 1\right] - \mathrm{I_{02}}\left[\exp\left(\frac{\mathrm{V} + \mathrm{R_s}l}{n_2 N_s V_t}\right) - 1\right] - \frac{\mathrm{V} + \mathrm{R_s}l}{\mathrm{R_{sh}}} \qquad (1.9)$$

In this context, the symbol N_s signifies the count of PV cells that are linked in a series connection. The electrical currents of multiple cells operating in parallel are denoted by I_{ph}, I_{01}, and I_{02}. The parameters Rs and R_{sh} describe the electrical resistances that arise from the practical implementation of the device. Specifically, R_s incorporates resistive losses that stem from both contact resistances and deviations from ideal semiconductor behaviour, while R_{sh} characterizes the leakage losses that occur in the p-n junctions. For optimal enhancement of the fill factor, it is advantageous to reduce the value of R_s while concurrently increasing R_{sh}.

Manufacturers of devices do not usually provide information on the seven unspecified parameters of the two-diode model, namely I_{ph}, I_{01}, I_{02}, n_1, n_2, Rs, and R_{sh}, in the device datasheet. As a result, these parameters have to be estimated through analytical or experimental means.

5.2 System Parameters

5.2.1 Sun Hours in Chalochasowa

Chalochasowa is situated within the Muchinga region, with the regional capital, Chinsali, being roughly 160 kilometers or 99 miles distant in a direct line. Moreover, the linear distance separating Chalochasowa from Zambia's capital, Lusaka, is about 773 kilometers or 480 miles. Chalochasowa experiences an annual average of 4400 hours of sunlight, with a daily average of 11.5 hours of sunlight. From June to November, the average daily sunlight hours are close to 12 hours, while from December to April, it's 11 hours per day. The average radiation is 4.2 kWh/m² per day [47]. The calculation of Insolation on an Inclined Plane was done using Lid and Jordan's equation.

$$K_T = \frac{H}{H_o}$$

$$H_o = \frac{24}{\pi} I_{sc}\left(1 + 0.033\cos\frac{360n}{365}\right)\left(\cos\emptyset\cos\delta\sin\omega_s + \frac{\pi\omega_s}{180}\sin\varphi\sin\delta\right) \qquad (2.0)$$

The location of a particular point can be determined using specific variables. These variables include I_{sc}, which represents the solar constant at 1367W/m2; n, which represents the day number of the year, Ø which represents the latitude; δ represents the solar declination; and ω_s represents the sunset hour angle.

$$23.5 \sin \frac{360(n + 284)}{365} \tag{2.1}$$

$$\omega_s = \cos^{-1}(-\tan \delta \tan \emptyset) \tag{2.2}$$

Figure 9: Satellite imagery delineating the study area within Chalochasowa. [30]

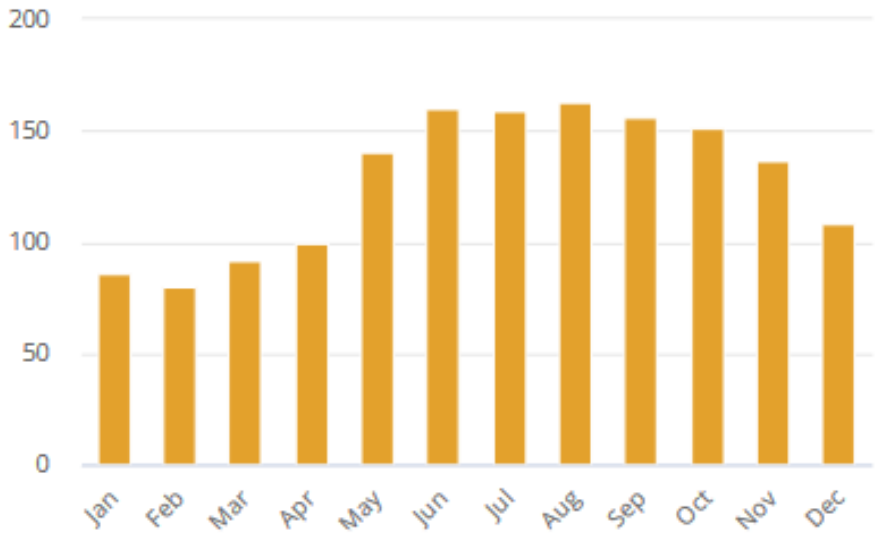

Figure 10: Monthly average solar insolation in Chalochasowa (kWh/m²). [30]

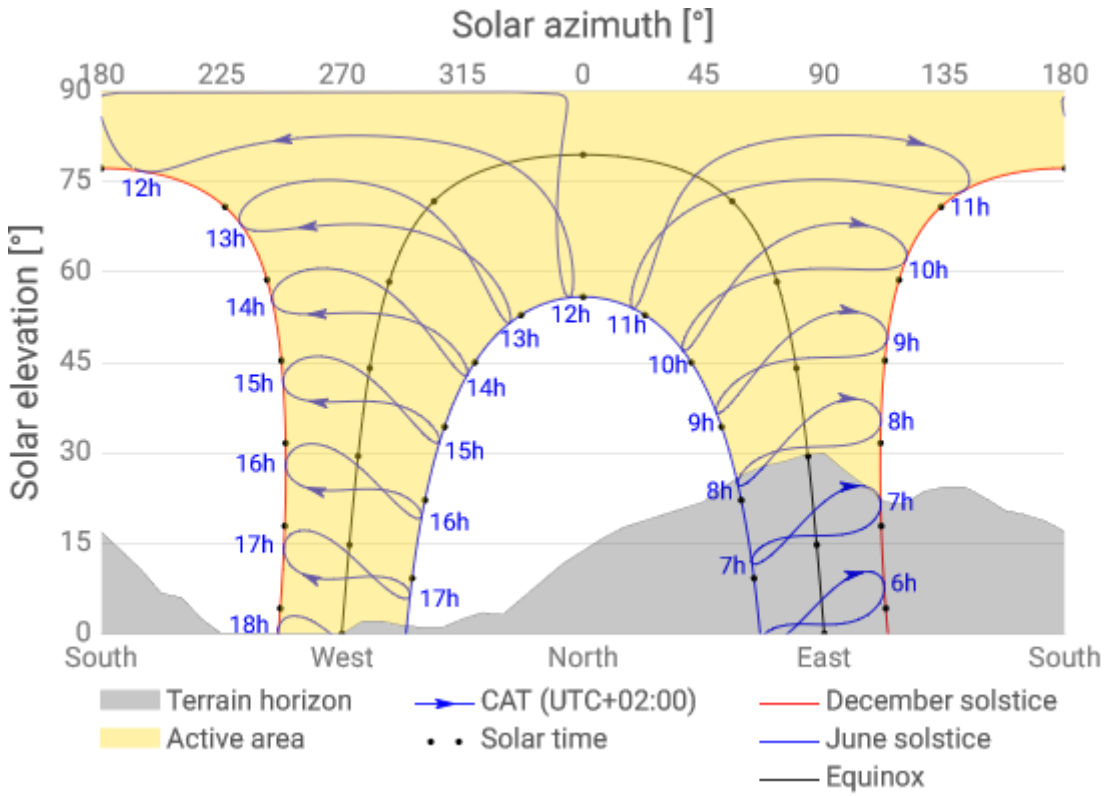

Figure 11: Sunpath diagram for Chalochasowa region, indicating solar azimuth and elevation throughout the year with terrain horizon overlay, providing critical data for solar energy studies and architectural design in relation to sunlight exposure. [30]

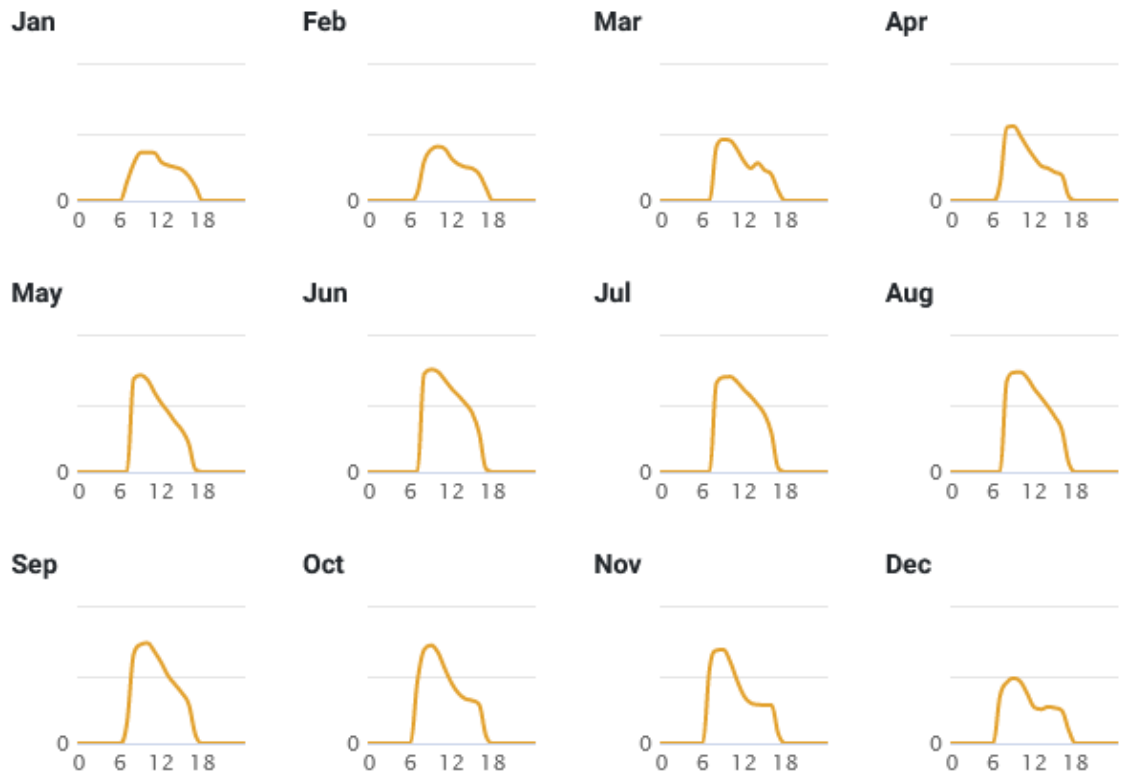

Figure 12: Average hourly profiles (Direct normal irradiation) in Chalochasowa (Wh/m²). [30]

5.2.1.1 The ideal angle for positioning solar panels (Optimal tilt angle)

To optimize the performance of solar panels, one should align them in a way that maximizes sunlight exposure. However, identifying the optimal orientation involves several factors. It's presumed that the panel is either stationary or capable of seasonal tilt adjustments. In the northern hemisphere, the ideal orientation is true south, and in the southern hemisphere, it's true north. For this study, the focus is on true north orientation. Notably, true north differs from magnetic north, necessitating a correction when using a compass for panel alignment, as the discrepancy varies by location. Key terms in this context include tilt angle, azimuth, and zenith angle. Tilt angle refers to the panel's inclination relative to the ground, affecting how sharply it's angled toward the horizon. The Azimuth angle represents the direction of incoming sunlight, and the Zenith angle is the measure of the sun's rays' deviation from the vertical axis [46]. Achieving the optimal tilt angle is vital for enhancing solar panel efficiency and energy output [45].

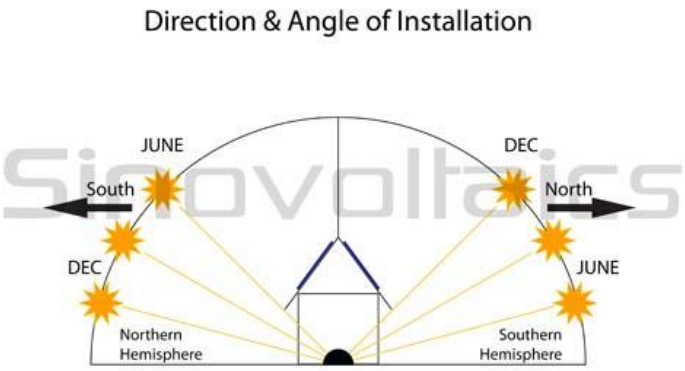

Figure 13: Illustrative diagram depicting the ideal angles and orientations for installing solar panels year-round in both the Northern and Southern Hemispheres, highlighting the necessary seasonal modifications to optimize solar energy absorption. [45]

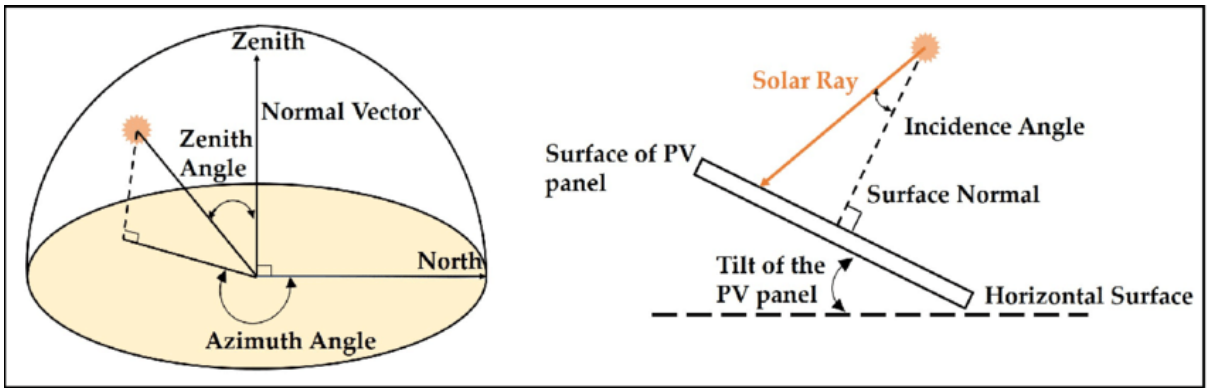

Figure 14: Azimuth angle, solar zenith angle, and geometry of the tilted surface. [46]

The ideal inclination (optimal tilt angle) of solar panels necessitates seasonal adjustments to maximize efficiency. The tilt angle should be increased by 15° during winters and reduced by 15° during summers. For this case, the angle of the latitude of Chalochasowa is taken (Chalochasowa latitude is 10.66 °). The calculated optimum tilt of PV modules from globalsolaratlas.info for the entire year of this region is 15°

5.2.2 Estimating Energy Consumption

When designing a stand-alone solar PV system, it's important to determine the total amount of energy needed each day. To estimate this, you must calculate the energy required by each appliance by measuring its power usage in watts and the number of hours it will be in operation. It's also necessary to consider the individual operating times for each load. After determining the daily energy needs, this data can be employed to ascertain the necessary dimensions of the solar panel array and the capacity of the battery storage system.

It's important to note that the energy consumption of appliances can vary depending on factors such as weather conditions and usage patterns. As such, it's recommended to add a safety margin to your energy estimates to ensure that your system can handle unexpected surges in energy consumption.

Additionally, the design of a stand-alone solar PV system should also take into account the location and orientation of the solar panels. Factors such as the latitude and longitude of the site, the angle of the sun, and any potential shading from nearby buildings or trees can all affect the efficiency of the system. It's important to carefully consider these factors during the design phase to maximize the system's performance. To determine the energy required by each appliance, you'll need to use its rating and the average number of hours it's used per day. The energy consumed by each load is measured in watt-hours (Wh), which can be calculated using the following equation:

$$E_i = P_i * T_u \tag{2.3}$$

The equation for calculating the energy demand per day of an individual load is based on three variables. The first variable, Ei, represents the energy demand in watt-hours. The second variable, Pi, refers to the rating of the load in watts. Lastly, Tu represents the time of use of the load per day, measured in hours. By plugging these variables into the equation, you can determine the energy demand of the load on a daily basis [22].

To determine the total amount of energy required on a daily basis, you must add up the individual energy demands for each appliance. This calculation will yield the daily total energy required for the system, as shown in Table 1. According to the figure, the total energy required each day is 7406 watt-hours (Wh) or 7.406 kilowatt-hours (kWh).

Around 23% of the required energy, which is equivalent to 1703.38 Wh, can be obtained directly from the solar panels. However, the remaining 77%, which is around 5702.62 Wh, will require energy storage for use during periods when solar energy is not available.

	Jan	Feb	Mar	Apr	May	Jun	Jul	Aug	Sep	Oct	Nov	Dec
0 - 1												
1 - 2												
2 - 3												
3 - 4												
4 - 5												
5 - 6												
6 - 7												
7 - 8	137	57		124					148	453	553	349
8 - 9	276	291	400	540	687	725	657	673	661	692	685	450
9 - 10	354	376	452	550	714	756	699	733	728	723	691	481
10 - 11	356	400	444	475	680	739	703	736	740	671	601	454
11 - 12	353	383	379	391	587	679	665	691	677	551	463	361
12 - 13	285	309	290	317	508	614	606	612	594	442	348	264
13 - 14	261	269	239	257	443	562	556	548	498	368	297	251
14 - 15	246	248	278	239	371	505	496	481	434	328	285	269
15 - 16	229	237	225	210	308	435	424	406	371	315	282	261
16 - 17	181	196	193	188	209	288	288	312	288	285	283	242
17 - 18	100	94	71	33	17	24	28	67	59	55	69	98
18 - 19												
19 - 20												
20 - 21												
21 - 22												
22 - 23												
23 - 24												
Sum	2778	2861	2970	3323	4525	5326	5123	5261	5196	4883	4557	3479

Figure 15: Required Daily Watt Hours [30]

5.2.2.1 Load Profile of Generic Residence in the Area

Table 1: The load profile of household appliances over a 24-hour period

Appliance	Quantity	Rating (Watts)	Usage per Day (Hours)	Total Energy per Day (Watt-hours)
TV	1	100	5	500
Cell Phone	3	4	6	72
Pressing Iron	1	1100	0.3	330
Incandescent Light Bulb	10	75	6	4500
Water Heating Element	1	1500	0.7	1050
Computer	1	50	2	100
Radio	1	5	4	20
Refrigerator	1	100	6	600
Mp3 player	2	1.5	2	6
Fan	1	54	2	108
Fluorescent Light	2	12	5	120
Total				7406

The load profile of a residence can be determined by itemizing all of the appliances in the residence and their corresponding wattage. In this case, the load profile of the residence is 7406 watt-hours per day. This information can be used to determine the size of the stand-alone PV power system needed to meet the residents' electricity needs.
The PV power system should be sized to generate enough electricity to meet the daily load profile, plus a margin of safety to account for days with cloudy weather or high electricity demand.

5.2.3 Sizing of the PV Array

Solar PV panels have varying power output depending on their ratings. The ratings are typically given in peak watts and are determined by the size of the module and the weather conditions of the location where they are installed. As a result, when calculating the number and size of PV panels needed to meet specific energy needs, it is important to consider the rated peak watts of the panels. This information is necessary to determine the appropriate number of panels needed to generate the required power output.

$$P_{t-pv} = \frac{E_t}{T_{peak-hours}} \times 1.3 \quad (3.2)$$

Where $P_{t\text{-}pv}$ is the complete size of the PV array in watts, $T_{peak\text{-}hours}$ is the lowest daily average peak-sun hours of a month in a year, and 1.5 represents the scaling factor. The system accounts for various losses, such as 77% panel efficiency, 85% storage battery efficiency, and 0.97% wiring system losses. Based on Figure 10, it was observed that the location experiences a minimum of 10 hours of sunshine per day during April, May, June, and July. As a result, the total peak power required for the location will be calculated.

$$P_{t-pv} = \frac{7406\text{Wh} \times 1.3}{10\text{h}} = 962.78\text{W} \quad (3.1)$$

Hence, the number of PV modules or panels required for the PV system is computed using the peak watts obtained in equation (3.3):

$$N_{\text{modules}} = \frac{P_{t-pv}}{Wp_i} \quad (3.3)$$

The equation uses two variables: $N_{modules}$, which represent the total number of modules, and W_{pi}, which is the power rating in peak watts of the chosen panel or module, measured in watts.

Or equation 3.4 can used,

$$N_{\text{modules}} = ((\frac{Watt\ hours\ per\ day}{\text{Sun Hours per day}})/\text{System Losses}))/250 \quad (3.4)$$

$$N_{\text{modules}} = ((\frac{7406\text{Wh}}{10\text{h}})/0.8)/250$$

$$N_{\text{modules}} = 3.703\ (4\ \text{Solar panels}\ 250\text{watts})$$

5.2.4 Battery system

5.2.4.1 Capacity of the Charge Controller

A charge controller, commonly referred to as a solar regulator, plays a vital role in a solar PV system, as it is essential for the appropriate charging of the batteries linked to the system. The fundamental function of a charge controller is to control the electrical charge flowing from the solar panels to the batteries, thereby averting scenarios of overcharging or excessive discharge of the batteries. In off-grid and hybrid solar PV systems, charge controllers serve a crucial role in orchestrating the distribution of electrical energy among solar panels, batteries, and loads. These controllers continuously monitor battery voltage and current, fine-tuning the charging process for optimal efficiency and safety.

They safeguard batteries against potential harm from overcharging or excessive discharging. Charge controllers are categorized into two types: PWM (Pulse-Width Modulation) and MPPT. PWM controllers, simpler in design, are typically employed in smaller systems. They manage battery charging by intermittently switching the solar panel output on and off, thereby maintaining a steady voltage. On the other hand, MPPT controllers are more advanced, enhancing solar panel power output by adjusting voltage and current in alignment with the battery's needs. This adjustment leads to more effective charging and improves overall performance of the solar PV system. [33].

The solar charge controller's rating is determined by its current and voltage. To calculate the current rating, one should use the short circuit current rating of the chosen PV modules, while the voltage should match the nominal voltage of the battery or batteries. Therefore, the ampere current rating for the solar charge controller can be determined through mathematical calculation as follows:

$$I_{scc} = I_{sc} \times 1.25 \tag{3.5}$$

The amperage of the solar charge controller is denoted as I_{scc}, while the short circuit current rating of the chosen PV unit is represented by I_{sc}. The value 1.3 signifies the safety margin. For our case, since the MTTP controller is recommended, we divide the total array wattage (1000W) by the battery bank nominal voltage (12V) to determine the charge controller's expected max output Amps.

For this scenario, the Outback Power System FLEXmax 60/80 was chosen as the suggested charge controller because it is very efficient.

Figure 16: FLEXmax 60/80 Charge Controller [42]

Table 2: FLEXmax 60/80 Charge Controller Specifications [42]

Models*:	FLEXmax 80 (FM80 to 150VDC)	FLEXmax 60 (FM60 to 150VDC)
Nominal Battery Voltages:	12, 24, 36, 48, or 60VDC (Single model, selectable via field programming at start-up)	12, 24, 36, 48, or 60VDC (Single model, selectable via field programming at start-up)
Maximum Output Current:	80A @ 104°F (40°C) with adjustable current limit	60A @ 104°F (40°C) with adjustable current limit
NEC Recommended Solar Maximum Array STC Nameplate:	**12VDC systems:** 1000W / **24VDC systems:** 2000W **48VDC systems:** 4000W / **60VDC systems:** 5000W	**12VDC systems:** 750W / **24VDC systems:** 1500W **48VDC systems:** 3000W / **60VDC systems:** 3750W
PV Open Circuit Voltage (VOC):	150VDC absolute maximum coldest conditions / 145VDC start-up and operating maximum	150VDC absolute maximum coldest conditions / 145VDC start-up and operating maximum
Standby Power Consumption:	Less than 1W typical	Less than 1W typical
Power Conversion Efficiency:	97.5% @ 80ADC in a 48VDC system (typical)	98.1% @ 60ADC in a 48VDC system (typical)
Peak Efficiency:	60VDC input w/48V battery at 53.1VDC (98.44%)	68VDC input w/48V battery at 52.8VDC (98.31%)
CEC Weighted Efficiency:	97.3% (at 48VDC)	97.3% (at 48VDC)
Charging Regulation:	Bulk, absorption, float, silent and equalization	Bulk, absorption, float, silent and equalization
Voltage Regulation Set Points:	13 to 80VDC user adjustable with password protection	13 to 80VDC user adjustable with password protection
Equalization Charging:	Programmable voltage setpoint and duration, automatic termination when completed	Programmable voltage setpoint and duration, automatic termination when completed
Battery Temperature Compensation:	Automatic with optional RTS installed / 5.0mV per °C per 2V battery cell	Automatic with optional RTS installed / 5.0mV per °C per 2V battery cell
Voltage Step-Down Capability:	Down convert from any acceptable array voltage to any battery voltage. **Example:** 72VDC array to 24VDC battery; 60VDC array to 48VDC battery	
Programmable Auxiliary Control Output:	12VDC output signal which can be programmed for different control applications (maximum of 0.2ADC)	12VDC output signal which can be programmed for different control applications (maximum of 0.2ADC)
Status Display:	3.1in (8cm) backlit LCD screen, 4 lines with 80 alphanumeric characters total	3.1in (8cm) backlit LCD screen, 4 lines with 80 alphanumeric characters total
Remote Display and Controller:	Optional MATE3s, MATE or MATE2	Optional MATE3s, MATE or MATE2
Network Cabling:	Proprietary network system using RJ-45 modular connectors with CAT5 cable (8 wires)	Proprietary network system using RJ-45 modular connectors with CAT5 cable (8 wires)
Data Logging:	**Last 128 days of operation:** amp-hours, watt-hours, time in float, peak watts, amps, solar array voltage, maximum battery voltage, minimum battery voltage and absorb time, accumulated amp-hours, and kWh of production	
Operating Temperature Range:	–40 to 60°C (power automatically derated above 40°C)	–40 to 60°C (power automatically derated above 40°C)
Environmental Rating:	Indoor Type 1	Indoor Type 1
Conduit Knockouts:	One 1in (25.4mm) on the back; One 1in (25.4mm) on the left side; Two 1in (25.4mm) on the bottom	One 1in (25.4mm) on the back; One 1in (25.4mm) on the left side; Two 1in (25.4mm) on the bottom
Warranty:	Standard 5 year, extended 10 year available	Standard 5 year, extended 10 year available
Weight (lb/kg):	**Unit:** 12.20 / 5.53 **Shipping:** 15.5 / 7	**Unit:** 11.65 / 5.3 **Shipping:** 14.9 / 6.8
Dimensions H x W x D (in/cm):	**Unit:** 16.25 × 5.75 × 4.5 / 41.3 × 14.6 × 11.4 **Shipping:** 19 × 9.5 × 8.5 / 48.3 × 24.1 × 21.6	**Unit:** 13.75 × 5.75 × 4.5 / 35 × 14.6 × 11.4 **Shipping:** 17 × 9.5 × 8.5 / 43.2 × 24.1 × 21.6

5.2.5.2 Sizing of the Battery Bank

Sizing the battery bank of a stand-alone solar PV system is a crucial aspect that requires careful consideration to ensure optimal performance and longevity of the system. The battery bank is responsible for storing excess energy generated by the PV panels during periods of peak solar irradiation and supplying this energy to loads during periods of low solar irradiation or no sunlight. The sizing of the battery bank is influenced by several factors, including the system's power demand, the daily load profile, the solar radiation availability, the battery technology, and the depth of discharge (DOD) required for the batteries [40]. The main factors are listed as follows.

a) The total energy required by the appliances during the absence of sun.
b) Days of autonomy
c) Discharge depth of battery and
d) The battery's nominal voltage

In this context, "days" refer to a consecutive number of cloudy days that may happen, during which the battery is responsible for providing energy to the load. It is common to consider a standard of 3 days for the duration of autonomy (D_{aut}). As a result, the battery capacity should be 1.5-3 times the calculated rating to ensure enough energy compensation during cloudy or rainy periods.

$$Ah_{bank} = \frac{E_t}{V_{dc-sys}} \times D_{aut} \times 1.25 \qquad (4.0)$$

Based on Table 1 appliances, given that the area receives an abundant amount of sun, we may not require energy storage for most of the time except the nights. Instead, appliances can be directly powered by the solar panel, which helps reduce the cost of the battery bank. Therefore, when calculating the storage battery bank's required energy capacity, the total energy taken into consideration in the design can be taken into account a little less, depending on the economic situation. In this case, the full capacity was considered. From the formula (4.0), $\mathrm{Ah}_{\mathrm{bank}}$ represents the capacity of the battery bank in Ah, and $\mathrm{V}_{\mathrm{dc-sys}}$ represents solar voltage in DC. In the calculation below, it was found that approximately 580Ah of battery capacity is required for the system.

$$\mathrm{Ah}_{\mathrm{bank}} = \frac{7406 \times 3 \times 1.25}{48\mathrm{V}} = 580\ \mathrm{Ah} \tag{4.1}$$

5.2.7 Inverter Sizing

The sizing of an inverter for a stand-alone solar PV system is an important stage in the design process. The inverter assumes responsibility for the conversion of direct current electrical energy emanating from solar panels into alternating current electrical energy, rendering it suitable for consumption by various electrical loads.

If the inverter is too small, it will not be able to give adequate power to the loads and may overheat or fail. If the inverter is too huge, it will be inefficient and waste energy.

As a result, the inverter must be capable of handling around 1kW at 220 volts. The inverter's input rating should be greater than the total wattage required of the appliance, plus a 25% safety buffer to accommodate for surge requirements, which are equal to 1.25 x 962.78W = 1.2kW as the precise number or 1.25kW as the approximate amount. The *Inverex Aerox* 1.2kW inverter was chosen for this application.

5.2.8 Calculation of Cable Size

In a stand-alone solar PV system, the sizing of cables is critical for optimal performance and system safety. Cable sizing is influenced by the system voltage, distance between the PV panels, battery bank, loads, and current capacity. The initial step in ascertaining the suitable cable size involves calculating the peak current produced by the system. This is determined by considering the total power output of the PV panels and the voltage of the system. The cable required for solar PV systems must be able to withstand exposure to both UV light and water and be suitable for use both indoors and outdoors. Low voltage systems, which often involve high current, have experienced issues with high voltage.

Additionally, since low-voltage systems typically involve high currents, it is important to use cables that are designed to handle these conditions. If the cables are not rated for the high currents, they can overheat and potentially cause a fire or damage the equipment. On the other hand, if the cables are not rated for the voltage levels that may be present, they can become damaged or degrade over time, leading to reduced efficiency or even system failure. As a result, it is necessary to determine

the size of the system appropriately to keep voltage drops below 2%. The calculation for voltage drops in a conductor carrying current is as follows:

$$V_d = \frac{\rho L I_{max}}{A} \tag{4.2}$$

The formula involves four variables: ρ, which represents the resistivity of the wire material in ohmmeters; L, the length of the cable; V_d, the maximum allowed voltage drops in the cable; and I_{max}, the maximum current that the cable can carry.

6. MATLAB Simulation of Designed PV System

MATLAB simulation is a powerful tool that can be used to analyse the performance of the designed off-grid PV system under different conditions. It can also be used to optimize the design of the system to improve its performance. Figure 12 shows the overall design of the system in Simulink.

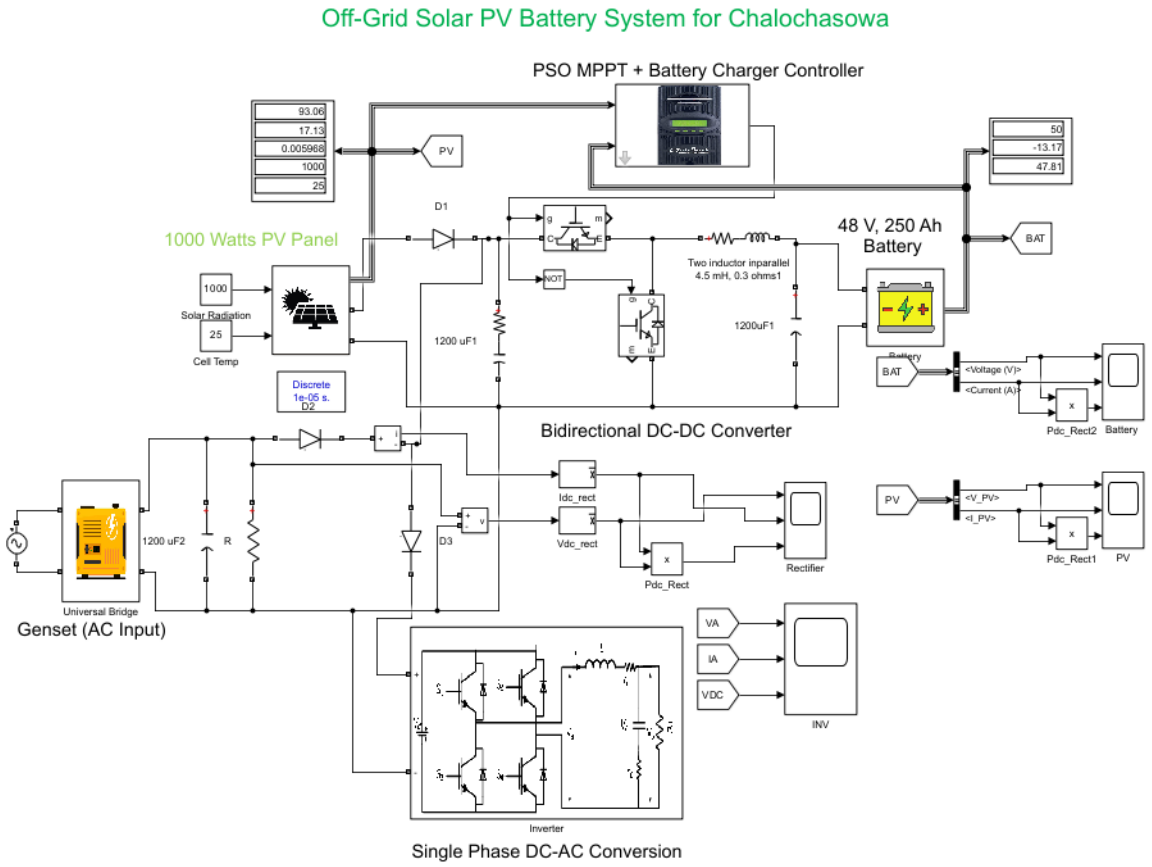

Figure 17: Overall designed simulation system in Simulink MATLAB for an off-grid solar PV battery system for Chalochasowa

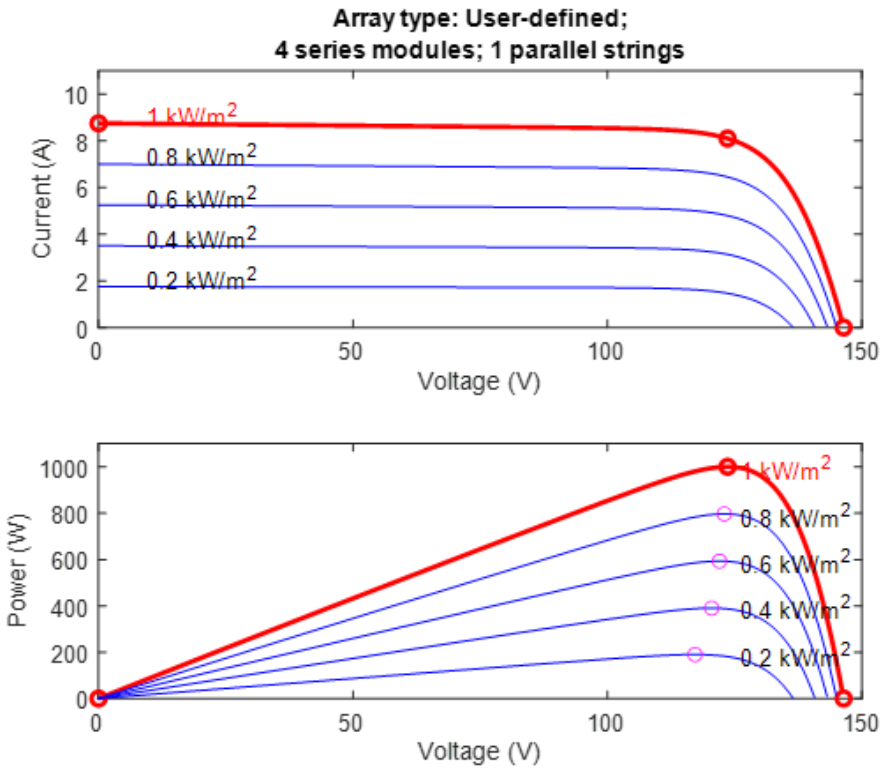

Figure 18: IV and PV curve of the solar PV panel. The peak power of solar panels varies with changes in irradiation.

The simulation model of this designed off-grid solar battery system consists of solar panels with a rating of 1000W. In the array of modules, every single panel has a rating of 250W in a four-series model and 1 parallel string, consequently giving a maximum power point voltage of 30.9V and corresponding current at the max of power point to be 8.1A.

With reference to Figure 12, the Solar PV output is connected to two components. The single-phase DC-AC Converter and the bidirectional DC-DC converter. The output connected to the single-phase DC-AC Converter is for the AC load (home load), while the output is connected to the battery through the bidirectional DC-DC converter for is used for charging the battery. For this condition, the implemented concept is that the Solar PV array first powers the AC load, and any access power is used to charge the battery. In the event that the solar PV output is zero, this means that the battery supplies the power to the AC load via the single-phrase DC-AC converter. In the event that neither the solar PV panel nor the battery can provide enough power for the load, a Genset (backup generation) can be used.

6.1 Simulation Battery Parameters

The type of battery used in the simulation is a Lead-Acid Battery. Simulink implements a generic battery model for the most popular battery types; therefore, the effects of temperature and aging (due to cycling) are already taken into consideration.

Type: Lead-Acid
Nominal voltage: 48V
Rated capacity: 250Ah
Initial state-of-charge: 50%
Battery response time: 30s

6.2 Inverter (Single Phase DC-AC Conversion)

The single-phase DC-AC converter is controlled by means of voltage current control. The "Voltage PI controller in Unbalance d-q control" applies the voltage control concepts, while the "Current inner loop PI control" applies the current control concepts. PWM generator and Half-Bridge (H-Bridge) inverter circuit.

The inverter from the block diagram, the converter starts with a DC power source either from the batteries or solar panels. The input DC is fed into a DC link or a DC bus capacitor (L1). This component smoothens the incoming DC voltage and helps maintain a stable DC voltage level, reducing voltage fluctuations and providing a continuous source of energy. The DC power is then applied to the inverter. The inverter uses pulse-width modulation (PWM) to generate an AC waveform. The output of the inverter is then filtered to remove any residual PWM noise.

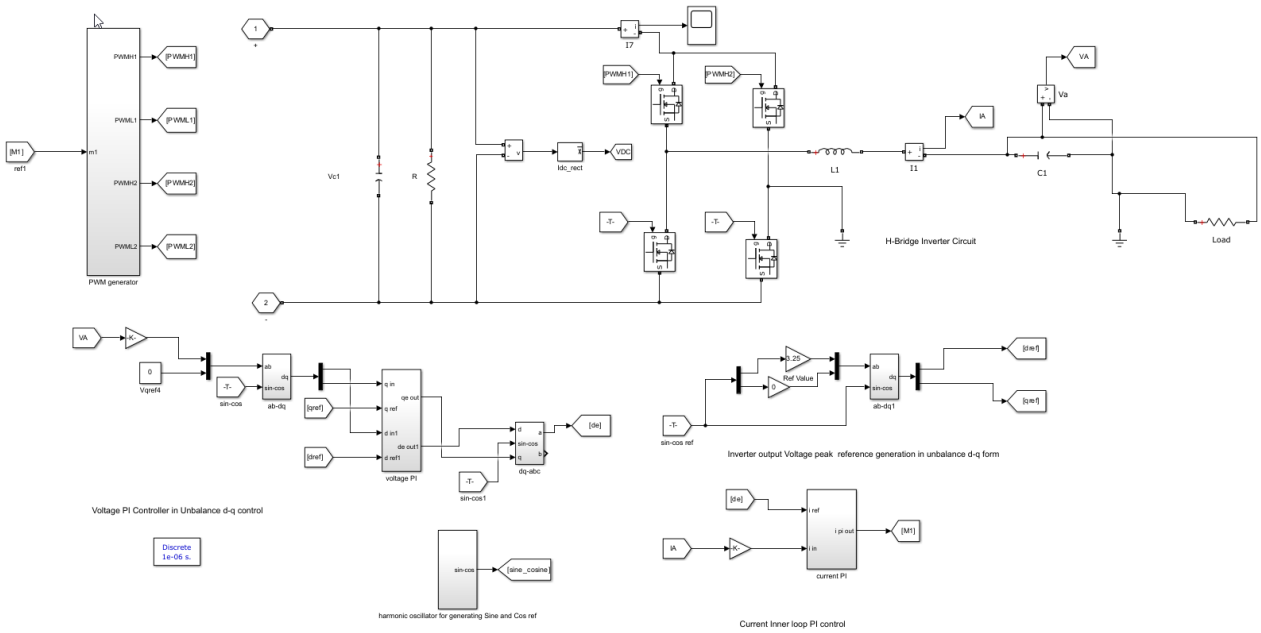

Figure 19: Overall Inverter (Single Phase DC-AC Conversion) Simulation

A clearer view of the H-Bridge inverter circuit, PWM generator, voltage, and current controller are shown in Figure 19.1-19.5

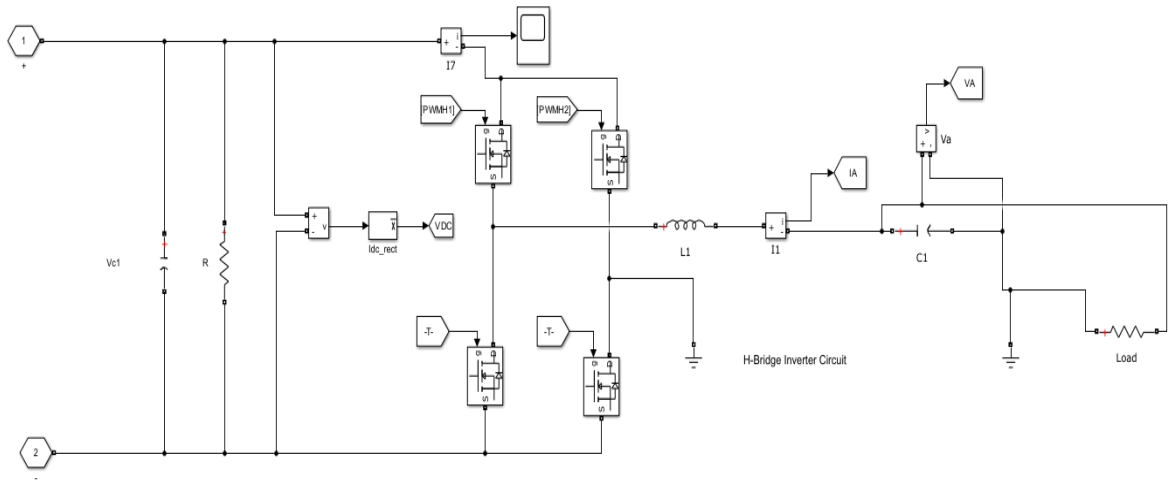

Figure 19.1: H-Bridge Inverter Circuit

The control method of the H-bridge's two parallel legs with two switches defines how it is used. The input to an H-bridge is a DC voltage source, and the output is also a DC voltage, but its magnitude and polarity can be regulated. The converter can be used to generate a square wave output voltage by closing switches PWMH1 and PWML2 at the same time while leaving PWMH2 and PWML1 open and then opening PWMH1 and PWML2 while closing PWMH2 and PWML1. If the duty cycle of both switch pairs is 50% and they are switched at the same time, the pulsed voltage waveform will be a perfect square wave of positive and negative polarity of the input DC voltage. Note that in this description, the PWMH1, PWMH2, PWML1, PWML2 are referring to the MOSFET transistors they are connected to in Figure 14.1.

Maintaining the same duty cycle for each switch pair but using a value other than 50% results in a pulse train with a value other than +Vdc for half of the cycle and Vdc for the other. Changing the duty cycle of one or both pairs of switches results in a variety of three-level output waveforms with 0 V output voltage for a portion of the cycle. This can also be accomplished by toggling PWMH1 and PWMH2 as a pair, as well as PWML2 and PWML1. To avoid a potentially dangerous short circuit of the input, also known as "shoot-through," switches in the same leg (PWMH1/ PWML1, PWMML2/ PWMH2) are typically not turned on and off at the same time in practice. To avoid this from happening, a short period of time known as "dead time" is employed to delay the activation of the opposing switches.

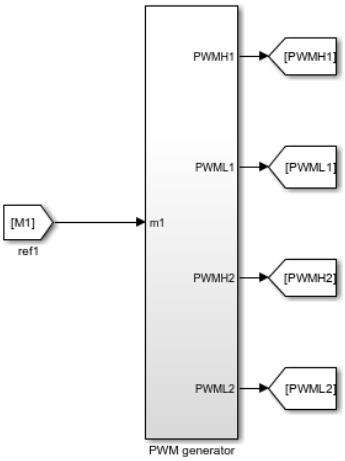

Figure 19.2: PMW Generator Model

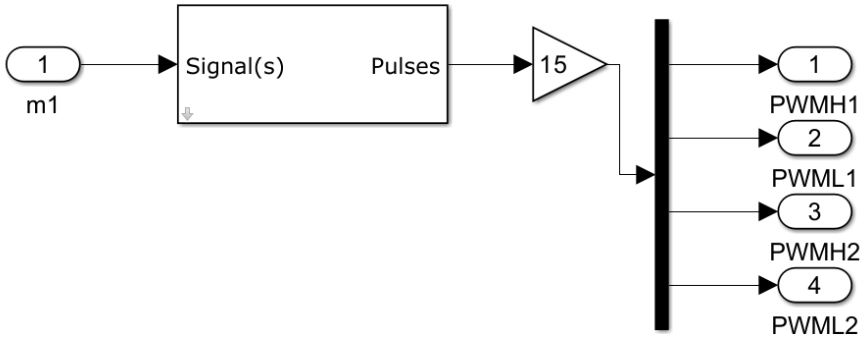

Figure 19.3: Inside the PMW Generator Model

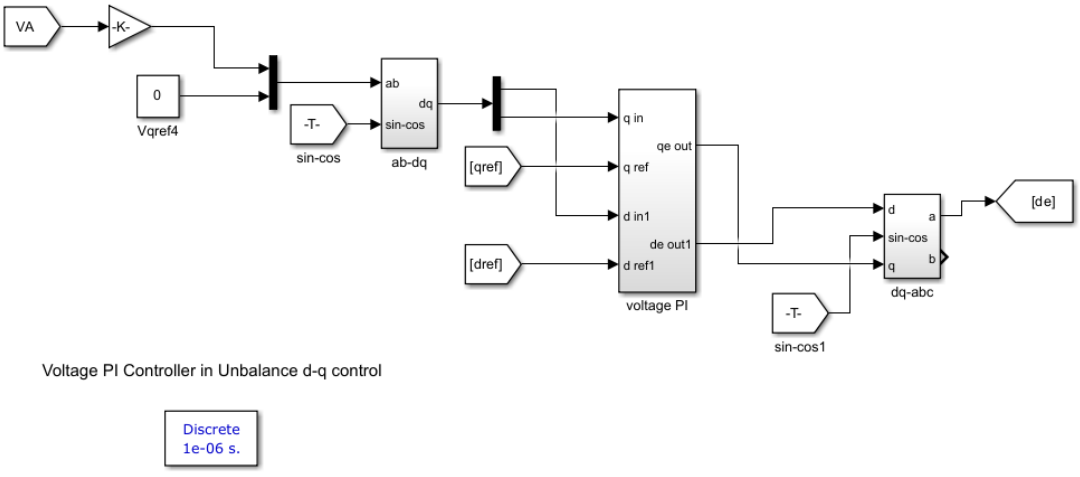

Figure 19.4: Voltage Control Model

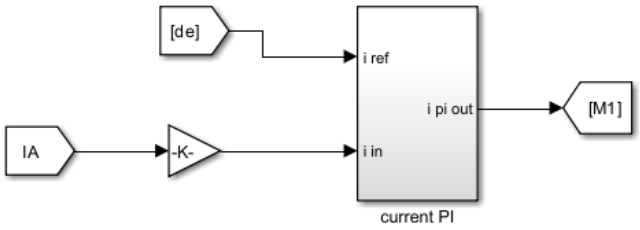

Figure 19.5: Current Control Model

6.3 PSO MPPT

Particle swarm optimization (PSO) is a metaheuristic algorithm inspired by the swarming behaviour of birds and fish. In PSO, a swarm of particles is initialized with random positions and velocities [52]. Each particle represents a candidate solution to the optimization problem [53]. The particles then move through the search space according to their velocities, which are updated based on the positions of the best-performing particles in the swarm. The algorithm terminates when a predefined stopping criterion is met or when a satisfactory solution is found. A PSO-based MPPT algorithm works by iteratively updating the duty cycle of the PV system's DC-DC converter to track the MPP. The duty cycle is the percentage of time that the DC-DC converter is turned on. By adjusting the duty cycle, the DC-DC converter can change the operating voltage of the PV array.

The PSO-based MPPT algorithm has several advantages over other MPPT algorithms, such as the perturb-and-observe (P&O) algorithm. The PSO algorithm is more robust to noise and partial shading conditions. It is also able to track the MPP more quickly and accurately than the P&O algorithm. This is why it was used in this simulation. The algorithm shown below (figure 20) works the following way:

I. Initialize a swarm of particles, with each particle representing a candidate duty cycle for the PV system's DC-DC converter.
II. Evaluate the fitness of each particle by measuring the current and voltage of the solar panel at that duty cycle and then calculating the output power of the PV system.
III. Update the velocity of each particle based on the positions of the best-performing particles in the swarm and the current and voltage of the solar panel.
IV. Update the position of each particle.
V. Repeat steps 2-4 until a predefined stopping criterion is met or when a satisfactory solution is found.

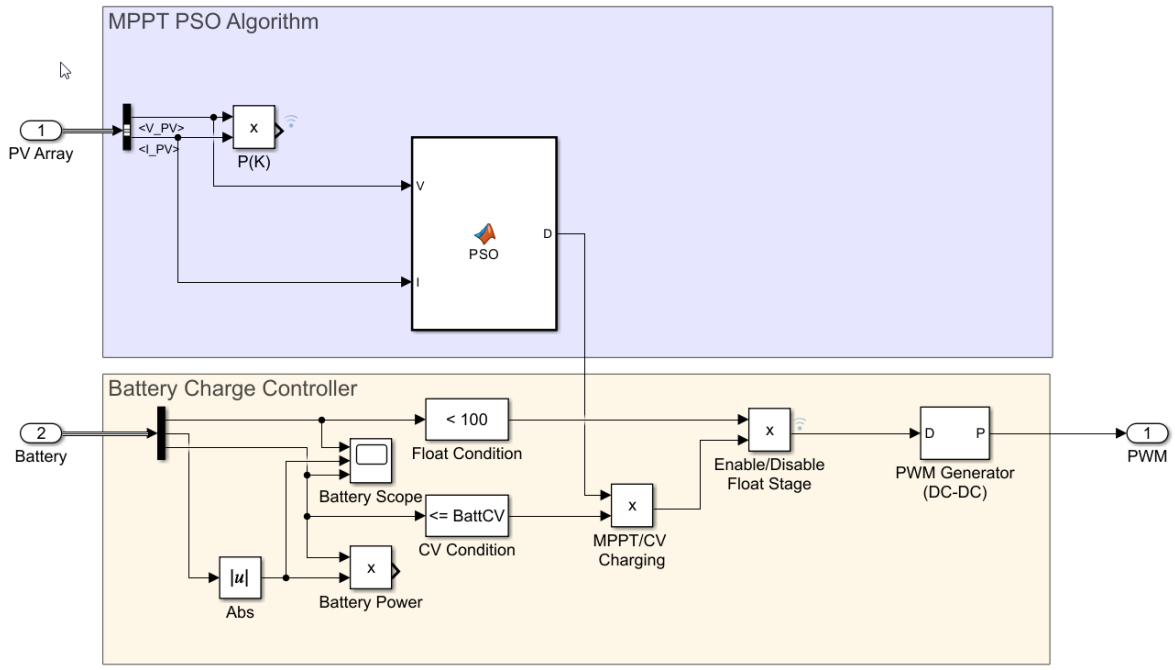

Figure 20: PSO MPPT and Charge Controller Simulation

6.4 Charge Controller

The battery charge controller uses the three-stage charging method, which consists of the constant current charging, constant voltage charging, and float charging stages. During the constant current phase of charging, the battery is subjected to a steady current flow until it attains a specified voltage level. This stage typically accounts for about 70% of the charging time. In the constant voltage charging phase, the battery undergoes charging at a stable voltage until it reaches full charge.

This stage typically accounts for the remaining 30% of the charging time. The charge controller simulation (Figure 15) begins by first measuring the voltage of the battery and the state of charge, then comparing it with the value of the float condition (<100) and the constant voltage. Based on this comparison, the algorithm will accept the duty cycle, or else it will block it.

6.5 Solar System Modes Simulation Results

6.5.1 Solar Power Mode (Full irradiation Mode Functionality)

In this instance, we make the irradiation to 1000 W/m^2 so as to simulate some irradiation to be experienced by the solar panel. This will be the normal working mode. The current, voltage, and power are referenced with regard to the PV, battery, Rectifier, and Inverter scope (Figure 21-21.3). Referencing Figure 21.1 (Battery Scope), it shows that the current and power are negative.

During this time of the simulation, the battery is undergoing charging (battery is in charging mode) as the solar panels are generating access power (The AC load continuously gets the power from the PV panel, and any excess charge is charging the battery). Lastly, backup power is not used; therefore, the rectifier current and voltage are zero (Figure 21.3). The scope simulation time used is 2 seconds for all the simulations.

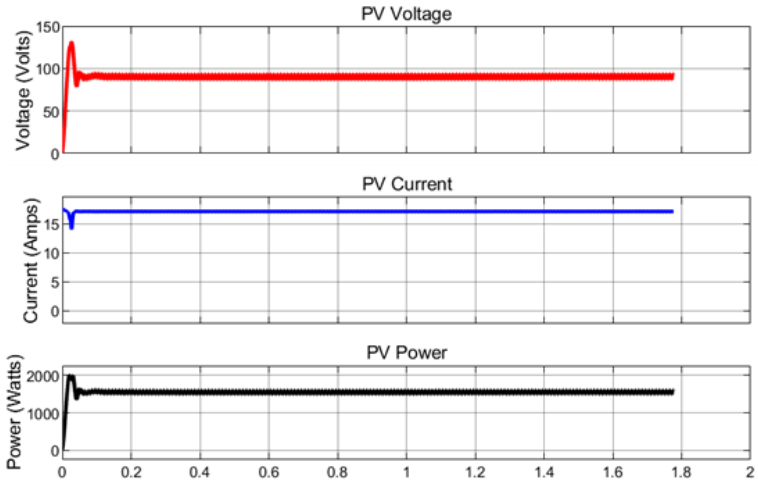

Figure 21: Simulated PV Voltage, Current and Power in Solar Power Mode

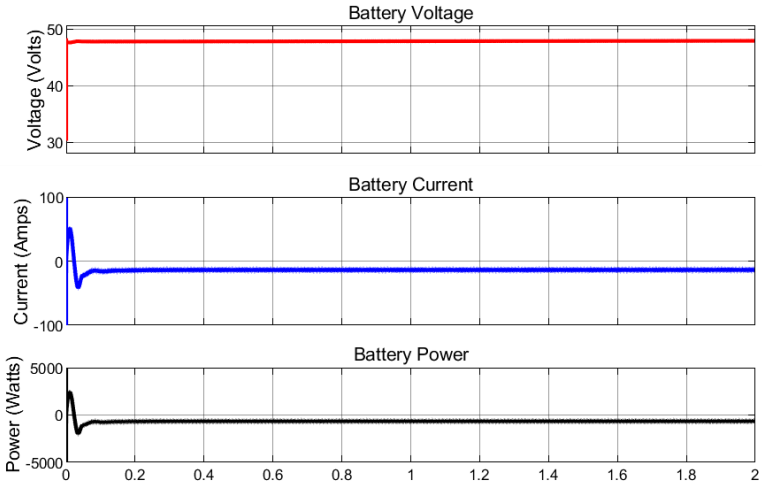

Figure 21.1: Battery Voltage, Current, and Power in Solar Power Mode

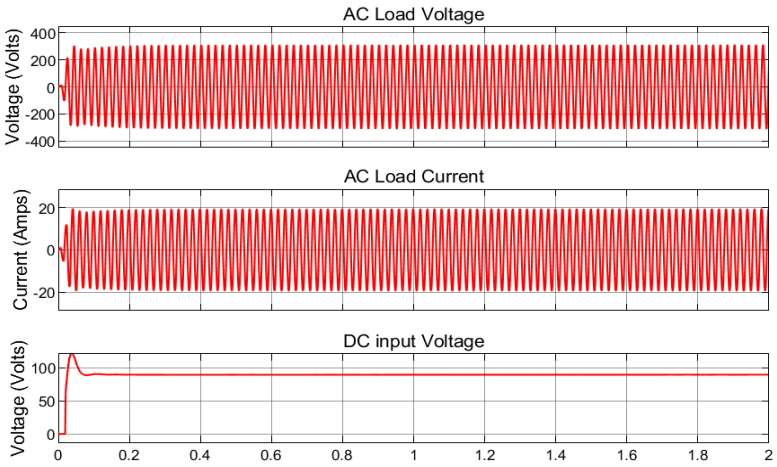

Figure 21.2: Simulated AC Load Voltage and Current in Solar Power Mode

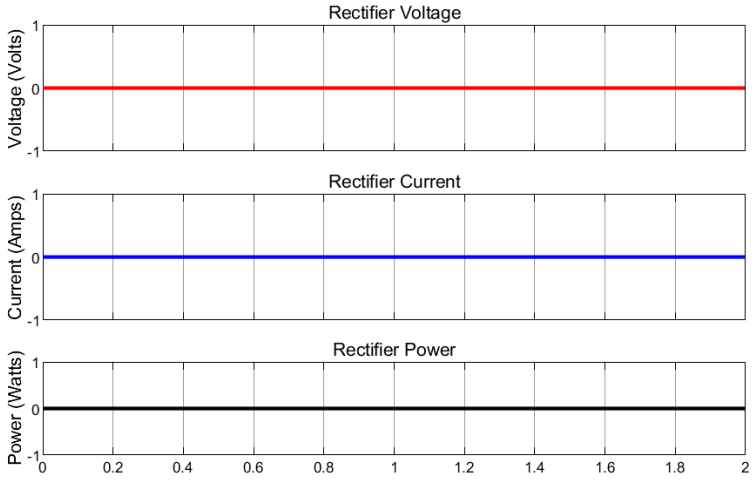

Figure 21.3: Simulated Rectifier Voltage, Current, and Power in Solar Power Mode

6.5.2 Battery Power Mode (No irradiation Mode Functionality)

In this instance, a simulation where there is no irradiation is done. This is done after 1 second of full irradiation. The solar panel value is set to zero; hence no, power has been generated, as seen in Figure 22. Theoretically, this scenario replicates conditions of dense cloud cover and foggy days or extreme solar heat, which could lead to overheating and inhibit power generation by the solar panels.

It is noticeable that the battery current shifts from negative to positive (as illustrated in Figure 22.2), transitioning from charging mode to active supply mode. It can also be observed that the AC load is continuously getting power from the battery. Rectifier output remains 0 as there is no direct AC input yet.

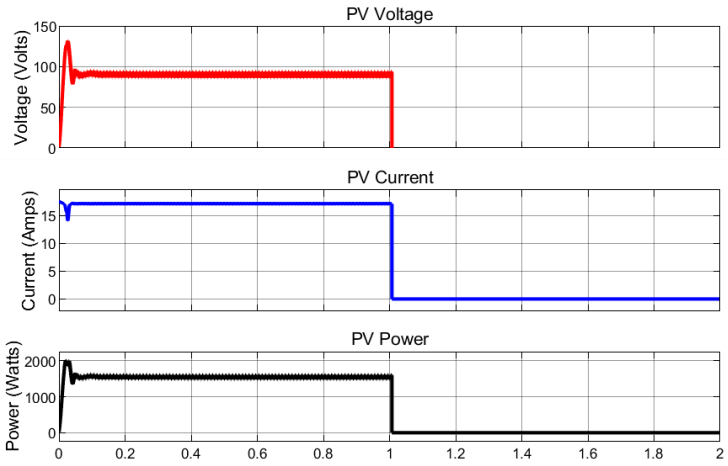

Figure 22: Simulated PV Voltage, Current, and Power in no irradiation mode (Between 1-2 Seconds)

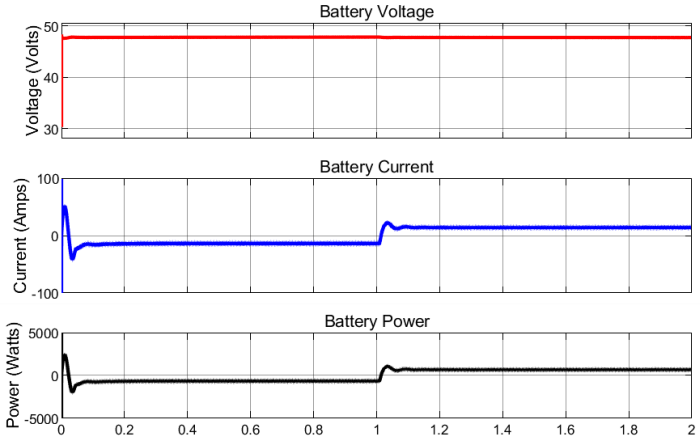

Figure 22.1: Battery Voltage, Current, and Power in no irradiation mode (Between 1-2 seconds)

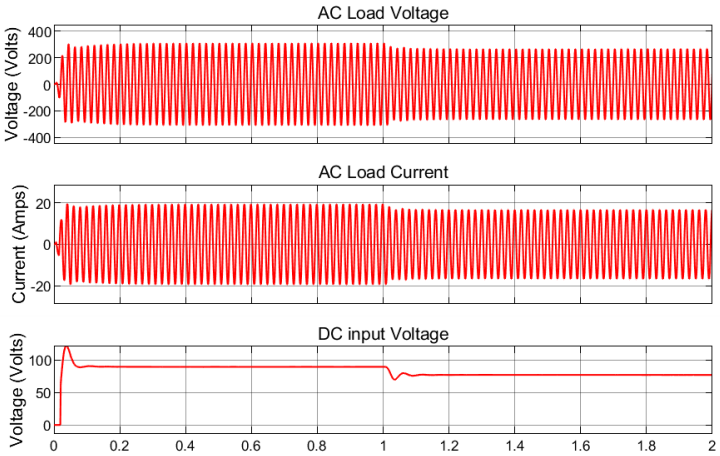

Figure 22.2: Simulated AC Load Voltage and Current

It can be observed in Figure 22 that the voltage goes a little below zero. This is caused by reverse bias. When a solar panel is connected to a load that is generating its own voltage, the solar panel can be forced into reverse bias. This means that the voltage applied to the solar panel is greater than the voltage that the solar panel is trying to produce. This happens when the solar panel is connected to a battery that is fully charged.

6.5.3 Genset Power Mode (No irradiation and No Battery Mode Functionality)

In this instance, we consider no irradiation and no battery power from the system. A backup generator is connected to the system. It can be observed that the generator is supplying the power to the system. (rectifier voltage is registered). The power generated from the generator directly powers the AC load; therefore, battery power will remain constant (Figure 23-23.2). A peak voltage amplitude of 123.6V is given from the generator.

It can also be observed that when we turn on both the backup generator and power from the solar panels for the system, the overall contribution of the generator is reduced.

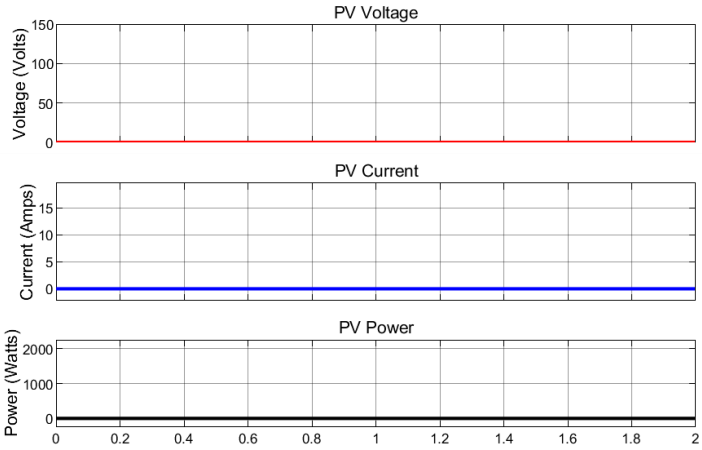

Figure 23: Simulated PV Voltage, Current, and Power in Solar Genset Power mode

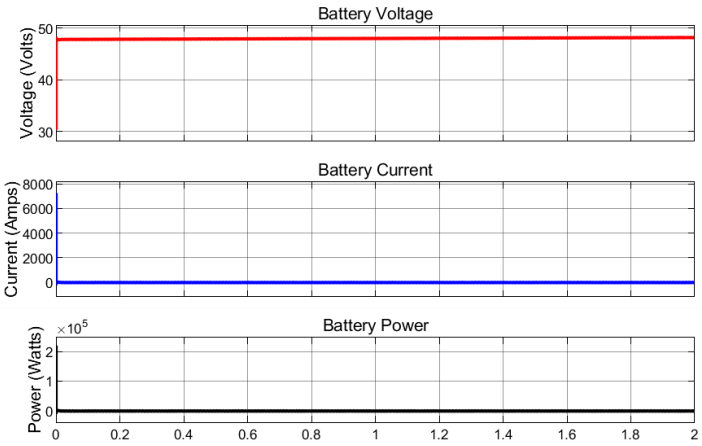

Figure 23.1: Battery Voltage, Current, and Power in Solar Genset Power Mode

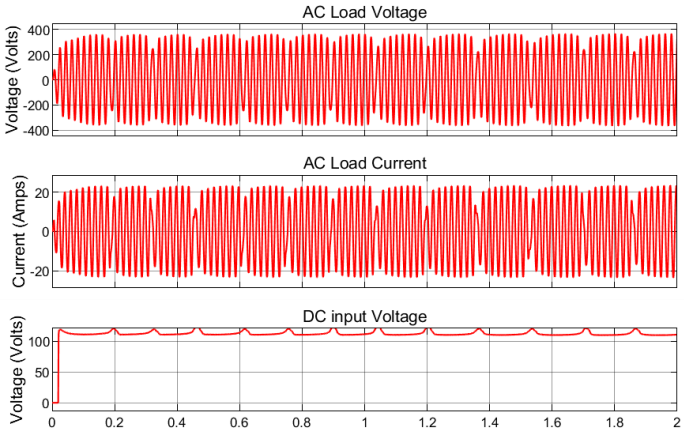

Figure 23.2: Simulated AC Load Voltage and Current

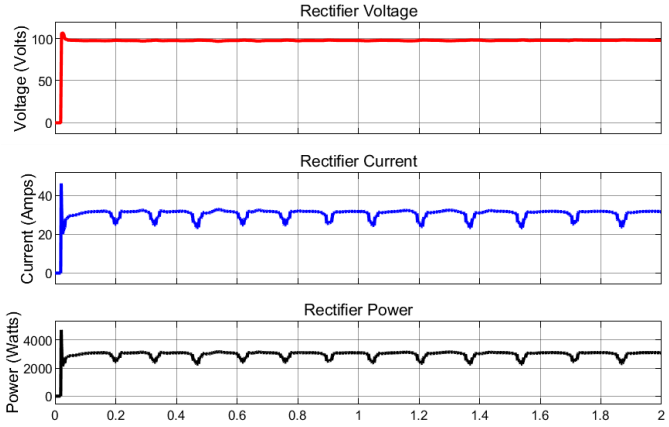

Figure 23.3: Simulated Rectifier Voltage, Current and Power in Genset Power Mode

7. System Efficiency Calculations

The efficiency of an off-grid PV system is a measure of how effectively it converts solar energy into usable electricity. This factor is of paramount importance in the design and operation of these systems, as it directly influences the electricity generation capacity and the overall economic efficiency of the system.

The overall efficiency of an off-grid PV system is the product of the efficiencies of its individual components, including solar panels, charge controllers, inverters, and batteries. Solar panel efficiency is typically the highest of these components, ranging from 15 to 20%. Charge controller and inverter efficiencies typically range from 75% to 98%, while battery efficiency can range from 70 to 96%.

To assess the effectiveness of a solar panel, quantified as a percentage, one should utilize the subsequent computation for estimation.

$$\text{Efficiency} = \frac{\text{Pmax}}{\text{Panel Area x Irradiance at STC}} \text{ x } 100$$

$$\text{Efficiency} = \frac{250\text{W}}{1.3761\text{m}^2 \text{ x } 1000\text{W/m}^2} \text{ x } 100$$

$$\text{Efficiency} = 18.17$$

- Pmax pertains to the solar module's electrical rating, measured in watts.
- Panel area specifies the physical dimensions of the solar module in meters. This step involves the computation of the module's surface area, expressed in square meters (m^2).
- The value of 1000 W/m² represents the commonly employed standard for the maximum solar irradiance, which serves as a reference when evaluating the power output of solar modules.

The operational effectiveness of a solar PV module is markedly contingent upon its exposed surface area, a determinant of its capacity to convert incident solar radiation into electrical power. The assessment of PV module efficiency necessitates a comparative scrutiny encompassing the solar irradiance absorbed from the sun and the ensuing electricity generation realized by the module. It is infeasible for a solar PV module to achieve the conversion of the entire incident solar irradiance into electricity, as such an outcome would imply an impractically idealized efficiency rate of 100%.

7.1 Charge Controller Efficiency

The efficacy of the charge controller holds significant importance as it delineates the quantum of solar energy transmuted into battery replenishment. MPPT charge controllers exhibit the potential to attain a charging efficiency exceeding 95%, albeit at a higher cost. In contrast, PWM charge controllers generally exhibit an efficiency of less than 80%, but they are relatively more cost-effective.

7.2 Battery Efficiency

Lithium-ion solar batteries exhibit rapid recharging capabilities and demonstrate superior efficiency in comparison to alternative battery chemistries, notably surpassing lead-acid and nickel-cadmium variants. They achieve a round-trip efficiency exceeding 96%, signifying that the proportion of electrical energy expended for the internal charging process is less than 4% of its total stored energy capacity. This characteristic presents dual advantages to end-users by diminishing costs and space requirements, as fewer solar panels are needed for power generation, and a reduced quantity of solar batteries is essential to provide requisite support, both in residential and commercial settings.

7.3 Inverter Efficiency

Inverter efficiency is conventionally quantified as the proportion of the functional AC output power relative to the aggregate of DC input power and any supplemental AC input power. Efficiencies of standard grid-connected inverters typically surpass 95% under a majority of operational conditions. This efficiency metric is subject to variations contingent upon factors such as AC output power, DC input voltage, and, occasionally, the temperature of the inverter itself.
The efficacy of an inverter is generally delineated as the quotient of the AC output power to the DC input power. Elevated levels of inverter efficiency are imperative for the optimization of energy extraction from solar PV systems. During this energy conversion process, certain losses are inevitable, manifesting primarily in two forms:

- Thermal dissipation (heat loss).
- Consumptive standby power is utilized to maintain the inverter in an operational state, also referred to as the inverter's no-load power consumption.

Accordingly, inverter efficiency can be represented by the equation efficiency= P_{AC}/P_{DC}, where P_{AC} denotes the AC output power in watts, and P_{DC} signifies the DC input power in watts. The typical range of inverter efficiency spans from 75% to 95%. This metric of power inverter efficiency is contingent on variations in inverter load capacity, with efficiency generally escalating and potentially reaching a peak at higher load capacities compared to lower ones, provided that the output power capacity of the inverter is not exceeded. It is noteworthy that at loading levels below 15%, the inverter efficiency is markedly reduced. Consequently, an optimal alignment between the inverter's capacity and its load can lead to enhanced efficiency, thereby yielding greater AC output power for the equivalent DC input.

7.4 Approximate Efficiency of the System.

Additional losses may occur due to wiring, which can collectively account for an additional 5% to 10% loss. This was taken as 5%. The approximate efficiency of the stand-alone system using the main components will be as follows:

Overall Efficiency = Efficiency of PV module × Efficiency of Charge Controller × Efficiency of Batteries × Efficiency of Inverter × Other losses.

Overall Efficiency = 0.18.17 × 0.85 × 0.96 × 0.80 x 0.95

Overall System Efficiency = 11.27%

Therefore, the approximate overall efficiency of a stand-alone PV system, considering average efficiencies for solar panels, charge controller, inverter, battery, and additional system losses, is about 11.2%. This value reflects the cumulative efficiency of converting sunlight into usable electrical energy in a stand-alone solar PV system.

8. Technical Issues Regarding Stand-Alone Solar Photovoltaic System

8.1 Intermittent PV Power Output

The principal challenge encountered in the application of PV systems pertains to the intermittency of power output. The integration of PV systems within the feeder infrastructure can introduce complications, manifesting as oscillations in power output, commonly referred to as voltage fluctuation within the electrical power system. Consequently, the electrical energy generated exhibits characteristics of inconsistency and instability. Power fluctuation is a phenomenon characterized by the erratic nature of the generated power, which arises due to obstacles impeding the reception of solar irradiance, thereby inducing variations in power production. Obstructions such as the transient passage of clouds contribute to the fluctuations in voltage.

The geographical placement and depth of integration of the PV system, along with the specific topological configurations adopted, exert discernible influences on the attributes of power output. Furthermore, suboptimal sizing of PV systems represents one of the primary causal factors contributing to the issue of voltage fluctuation [39]. PV systems characterized by diminished power absorption capacities inevitably reduce the quantity of power that can be effectively stored.

8.2 Variable Shading Conditions

Intermittently, the PV system experiences diminished power output due to factors such as mismatch and partial shading conditions. This phenomenon arises from dynamic elements such as drifting cloud cover, the obstruction of sunlight by natural and man-made objects, and overcast weather conditions, leading to non-uniform solar irradiance distribution across the PV array. As a consequence of these conditions, partial shading emerges, giving rise to local and global extrema within the system's power-output profile, thereby impacting the overall reliability of power generation. The power-versus-voltage characteristics of the PV array during partial shading conditions are depicted in the figure below.

Notwithstanding these challenges, the amelioration of partial shading conditions can be pursued through various means, including reconfiguring the arrangement of PV panels, employing structural frameworks, optimizing converter circuit topologies, or adopting MPPT techniques. Among these strategies, improving MPPT methods is particularly attractive owing to its inherent benefits, including straightforward implementation, cost efficiency, and smooth integration with existing systems. This rationale underscores the motivation for the simulation of MPPT algorithms using MATLAB Simulink, as elucidated in the preceding chapter [40].

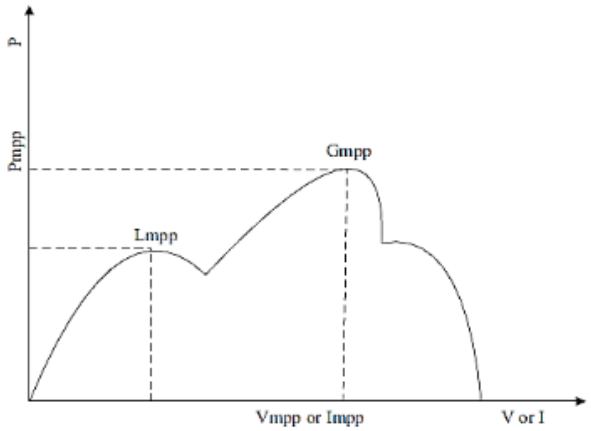

Figure 24: PV array's power characteristic under partial shading circumstances [40]

8.3 Photovoltaic Cells' Inability to Function at Elevated Temperatures

The thermal management of PV panel systems represents a pivotal concern in both their design and operational phases, as the overall efficacy of solar panels is profoundly contingent upon the thermal conditions experienced by PV cells. The manifestation of issues such as current mismatching and hot spots can be attributed to the presence of elevated and non-uniform cell temperatures, thereby precipitating a reduction in the efficiency of PV panels. Of particular consequence, the open-circuit voltage is notably affected by temperature escalation. The heightened thermal profile of PV cells stands as a detriment to their performance. In practical terms, only a limited portion, approximately 15-20%, of incident solar irradiation can be successfully converted into electrical energy, with the remaining portion dissipating as thermal energy. Moreover, this temperature-induced rise in electrical resistance within the circuitry exerts an adverse impact on the electron conversion rate, leading to diminished efficiency. Furthermore, the increase in PV cell temperatures can potentially have detrimental impacts on the properties of the materials used in the construction of solar cells [41]. Thus, it becomes evident that the establishment of a uniform and effective cooling system is imperative not only to optimize the operational performance of PV panels but also to extend their operational lifespan.

Conclusion

For a typical house in a rural area in Chalochasowa, the complete modelling, sizing, and optimization of an off-grid independent or stand-alone solar PV system was presented in this thesis. The designed system consists of 1000W PV, three batteries of 250 Ah, and a 1.5kW inverter. This thesis further presented an important simulation model to be implemented in Chalochasowa and anywhere else with similar solar conditions. The simulation was conducted using MATLAB/Simulink, version R2023a.
The experimental model underwent evaluation in three distinct scenarios. Initially, it was assessed under standard operational parameters of the PV system, focusing on its power generation capabilities. Subsequently, the model was examined in a scenario devoid of irradiation, where neither solar energy nor battery power was available to supply the load. In this instance, the system's performance was observed when either a generator set (Genset) or an AC power source was integrated into the system.

The simulation of the stand-alone PV solar system in MATLAB Simulink was successful in all three conditions. The system successfully tracked the maximum power point of the PV array, maintained the DC bus voltage, and supplied power to the load, adapting to varying conditions of solar irradiation and load demands. The simulation results also showed that the system was stable and robust to disturbances. These findings indicate that the proposed simulation model is applicable for designing and analysing stand-alone PV solar systems across a diverse range of applications. The model can also be used to evaluate the performance of different MPPT algorithms and converter control strategies. Furthermore, efficiency calculations of the system based on overall efficiencies were carried out. It is important to note that the efficiency of the stand-alone PV solar system is influenced by various factors, including the design and quality of PV modules, the capacity of the energy storage system, and the overall system architecture. This analysis underscores the significance of optimizing these components to maximize system efficiency and, consequently, the return on investment for such systems.

The implementation of stand-alone PV systems in remote areas of developing countries like Zambia is an important strategy for addressing the challenges of energy poverty and environmental sustainability. These systems are capable of delivering dependable and environmentally friendly electricity to communities off the grid, diminishing dependency on fossil fuels, generating employment opportunities, and enhancing the local economy.

References

[1]. Iea. People without access to electricity worldwide, 2012-2022 – charts – Data & Statistics, IEA. Available at: https://www.iea.org/data-and-statistics/charts/people-without-access-to-electricity-worldwide-2012-2022 (Accessed: 20 June 2023).

[2]. Environmental and Energy Study Institute (EESI), Fact sheet: Climate, environmental, and health impacts of fossil fuels (2021), EESI. Available at: https://www.eesi.org/papers/view/fact-sheet-climate-environmental-and-health-impacts-of-fossil-fuels-2021 (Accessed: 20 June 2023).

[3]. 26, M.E. |October et al. (2022) Solar panels reduce CO2 emissions more per acre than trees - and much more than corn ethanol, State of the Planet. Available at: https://news.climate.columbia.edu/2022/10/26/solar-panels-reduce-co2-emissions-more-per-acre-than-trees-and-much-more-than-corn-ethanol/ (Accessed: 20 June 2023).

[4]. Kruger, W. and Eberhard, A. (2018) 'Renewable energy auctions in sub-saharan Africa: Comparing the South African, Ugandan, and Zambian programs', WIREs Energy and Environment, 7(4). doi:10.1002/wene.295.

[5]. (2022) U.S. Agency for International Development. Available at: https://www.usaid.gov/powerafrica/zambia (Accessed: 20 June 2023).

[6]. Samboko, P.C. et al. (no date) Load shedding and charcoal use in Zambia: What are the implications on ..., Load shedding and charcoal use in Zambia: What are the implications on forest resources. Available at: https://www.researchgate.net/profile/Paul-Samboko 2/publication/314395465_Load_shedding_and_charcoal_use_in_Zambia_What_are_the_implications_on_forest_resources/links/58c1708a92851c2adfeebee8/Load-shedding-and-charcoal-use-in-Zambia-What-are-the-implications-on-forest-resources.pdf (Accessed: 20 June 2023).

[7]. Rooij, D.D. (2023) Islanding: What is it and how to protect from it?, Manage risks and maximize ROI for your PV and energy storage projects. Available at: https://sinovoltaics.com/learning-center/system-design/islanding-protection/ (Accessed: 20 June 2023).

[8]. Michał (no date) Island operation, Emissions. Available at: https://emissions-euets.com/internal-electricity-market-glossary/634-island-operation (Accessed: 20 June 2023).

[9]. Ahsan, S. et al. (2016) 'Design and cost analysis of 1KW photovoltaic system based on actual performance in Indian scenario', Perspectives in Science, 8, pp. 642–644. doi:10.1016/j.pisc.2016.06.044.

[10]. S. HIWALE, DR.A., V.PATIL, M. and VINCHURKAR, H. (2014) 'An efficient MPPT solar charge controller', International Journal of Advanced Research in Electrical, Electronics and Instrumentation Engineering, 3(7), pp. 10505–10511. doi:10.15662/ijareeie.2014.0307017.

[11]. Oko, C. et al. (2012) 'Design and economic analysis of a photovoltaic system: A case study', International Journal of Renewable Energy Development, 1(3), p. 65. doi:10.14710/ijred.1.3.65-73.

[12]. Sasu, D.D. (2023) Zambia: Total renewable energy capacity 2012-2021, Statista. Available at: https://www.statista.com/statistics/1316240/total-renewable-energy-capacity-in-zambia/ (Accessed: 08 July s2023).

[13]. Nisa, Z.U. (2017) 4 th International Conference on Energy, Environment and Sustainable Development, Academia.edu. Available at:

https://www.academia.edu/35234799/4_th_International_Conference_on_Energy_Environment_and_Sustainable_Development (Accessed: 08 July 2023).
[14]. The Sun and the seasons (no date) Understanding Astronomy: The Sun and the Seasons. Available at: https://physics.weber.edu/schroeder/ua/SunAndSeasons.html (Accessed: 08 July 2023).
[15]. Armstrong, S., Glavin, M.E. and Hurley, W.G. (2008) 'Comparison of battery charging algorithms for Stand Alone Photovoltaic Systems', 2008 IEEE Power Electronics Specialists Conference [Preprint]. doi:10.1109/pesc.2008.4592143.
[16]. Singh, G., Sokana, M.Y. and Nouhou, S.A. (no date) Renewables readiness assessment: Zambia. Available at: https://www.irena.org/-/media/Files/IRENA/Agency/Publication/2013/RRA_Zambia.pdf (Accessed: 08 July 2023).
[17]. Bowa, K.C. et al. (no date) Solar photovoltaic energy progress in Zambia : a review, Ujcontent.uj.ac.za. Available at: https://ujcontent.uj.ac.za/esploro/outputs/conferencePaper/Solar-photovoltaic-energy-progress-in-Zambia/9911845907691 (Accessed: 08 July 2023).
[18]. Glavin, M. and Hurley, W.G. (2006) 'Battery Management System for Solar Energy Applications', Proceedings of the 41st International Universities Power Engineering Conference [Preprint]. doi:10.1109/upec.2006.367719.
[19]. Basics of MPPT Solar Charge Controller (no date) Basics of maximum power point tracking (MPPT) Solar Charge Controller. Available at: https://www.leonics.com/support/article2_14j/articles2_14j_en.php (Accessed: 09 July 2023).
[20]. Tutorials, A.E. (no date) Grid connected PV system connects PV panels to the grid, Alternative Energy Tutorials. Available at: https://www.alternative-energy-tutorials.com/solar-power/grid-connected-pv-system.html (Accessed: 08 July 2023).
[21]. Ali, W. et al. (2018) 'Design considerations of stand-alone Solar Photovoltaic Systems', 2018 International Conference on Computing, Electronic and Electrical Engineering (ICE Cube) [Preprint]. doi:10.1109/icecube.2018.8610970.
[22]. SADC Regional Indicative Strategic Development Plan (RISDP) 2020–2030 (no date) Southern African Development Community. Available at: https://www.sadc.int/sites/default/files/2021-08/RISDP_2020-2030.pdf (Accessed: 08 July 2023).
[23]. Mertens, K. (2019) Photovoltaics: Fundamentals, technology and Practice. Chichester, West Sussex: Wiley.
[24]. Jäger, K.-D. et al. (2016) Solar Energy: Fundamentals, Technology and Systems. Cambridge: UIT Cambridge.
[25]. Sustainable energy for all | sustainable energy for all (no date) THE UNITED REPUBLIC OF TANZANIA MINISTRY OF ENERGY AND MINERALS. Available at: https://www.seforall.org/sites/default/files/TANZANIA_AA-Final.pdf (Accessed: 08 July 2023).
[26]. Crystalline silicon photovoltaics (no date) Crystalline Silicon Photovoltaics. Available at: https://www.pilkington.com/en/global/knowledge-base/types-of-glass/solar-energy/solar-technologies/crystalline-silicon-photovoltaics# (Accessed: 08 July 2023).
[27]. Gaikwad, Mr.K. (2020) 'Materials for solar energy', International Journal for Research in Applied Science and Engineering Technology, 8(8), pp. 827–830. doi:10.22214/ijraset.2020.31036.

[28]. Vinod, Kumar, R. and Singh, S.K. (2018) 'Solar Photovoltaic Modeling and Simulation: As a renewable energy solution', Energy Reports, 4, pp. 701–712. doi:10.1016/j.egyr.2018.09.008.
[29]. Silvestre, S. (2018) 'Strategies for fault detection and diagnosis of PV systems', Advances in Renewable Energies and Power Technologies, pp. 231–255. doi:10.1016/b978-0-12-812959-3.00007-1.
[30]. Solargis Global solar atlas. Available at: https://globalsolaratlas.info/map (Accessed: 08 July 2023).
[31]. Green, M.A. (2006) Third generation photovoltaics advanced solar energy conversion. Berlin: Springer.
[32]. Mourya, A. et al. (2022) 'Solar: Science of entity loss attribution', Proceedings of the 28th ACM SIGKDD Conference on Knowledge Discovery and Data Mining [Preprint]. doi:10.1145/3534678.3539087.
[33]. Ashok Kumar, L., Albert Alexander, S. and Rajendran, M. (2021) 'Charge controls and maximum power point tracking', Power Electronic Converters for Solar Photovoltaic Systems, pp. 331–369. doi:10.1016/b978-0-12-822730-5.00008-8.
[34]. Kumar, V. (2023) Zambia River Map, MapsofWorld.com. Available at: https://www.mapsofworld.com/zambia/river-map.html (Accessed: 08 July 2023).
[35]. Kachapulula-Mudenda, P. et al. (2018) 'Review of renewable energy technologies in Zambian households: Capacities and barriers affecting successful deployment', Buildings, 8(6), p. 77. doi:10.3390/buildings8060077.
[36]. Ministry of Mines, Energy and Water Development Public Disclosure ... Available at: https://documents.worldbank.org/curated/en/609911468334908943/pdf/E4134v200P1149 0017020130Box374335B.pdf (Accessed: 08 July 2023).
[37]. Mwanza, M. et al. (2017) 'Assessment of solar energy source distribution and potential in Zambia', Periodicals of Engineering and Natural Sciences (PEN), 5(2). doi:10.21533/pen.v5i2.71.
[38]. Inverex AEROX 1.2 KW - CITYUPS. Available at: https://cityups.com.pk/product/inverex-aerox-1-2-kw/ (Accessed: 14 November 2023).
[39]. Author links open overlay panelPriti Das et al. (2017) Modeling and characteristic study of solar photovoltaic system under partial shading condition, Materials Today: Proceedings. Available at: https://www.sciencedirect.com/science/article/abs/pii/S2214785317320795 (Accessed: 14 October 2023).
[40]. Saravanan, S. and Ramesh Babu, N. (2016) 'Maximum power point tracking algorithms for Photovoltaic System – A Review', Renewable and Sustainable Energy Reviews, 57, pp. 192–204. doi:10.1016/j.rser.2015.12.105.
[41]. Hasanuzzaman, M. et al. (2016) 'Global Advancement of Cooling Technologies for PV systems: A Review', Solar Energy, 137, pp. 25–45. doi:10.1016/j.solener.2016.07.010.
[42]. FLEXmax 60 / 80 (no date) FLEXmax 60/80 - Outback Power Inc. Available at: https://www.outbackpower.com/products/charge-controllers/flexmax-60-80 (Accessed: 14 October 2023).
[43]. Energy sector (2021) GET.invest. Available at: https://www.get-invest.eu/market-information/zambia/energy-sector/ (Accessed: 13 December 2023).
[44]. Machrafi, H. (2012) Green Energy and Technology. Sharjah, U.A.E: Bentham Science Publishers.
[45]. Rooij, D.D. (2023) Solar panel angle: How to calculate solar panel tilt angle?, Manage risks and maximize ROI for your PV and energy storage projects. Available at:

https://sinovoltaics.com/learning-center/system-design/solar-panel-angle-tilt-calculation/ (Accessed: 1 December 2023).
[46]. Masoom, A. et al. (2020) 'Rooftop Photovoltaic Energy Production Management in India using Earth-observation data and modelling techniques', Remote Sensing, 12(12), p. 1921. doi:10.3390/rs12121921.
[47]. Tutiempo Network, S.L. Hours of sunlight on Earth, www.tutiempo.net. Available at: https://en.tutiempo.net/daylight-hours/ (Accessed: 5 December 2023).
[48]. Travels in Geology: Tracking African animals and deranged drainages across the Kalahari (no date) Travels in geology: Tracking African animals and deranged drainages across the Kalahari. Available at: https://www.earthmagazine.org/article/travels-geology-tracking-african-animals-and-deranged-drainages-across-kalahari/ (Accessed: 13 December 2023).
[49]. Dobruszkes, F., Decroly, J.-M. and Suau-Sanchez, P. (2022) 'The monthly rhythms of Aviation: A Global Analysis of Passenger Air Service seasonality', Transportation Research Interdisciplinary Perspectives, 14, p. 100582. doi:10.1016/j.trip.2022.100582.
[50]. Routray, A. and Hur, S.-H. (2022) 'Leakage current mitigation of photovoltaic system using optimized predictive control for improved efficiency', Applied Sciences, 12(2), p. 643. doi:10.3390/app12020643.
[51]. Singh, J. (2023) Diode, Physics. Available at: https://www.concepts-of-physics.com/modern/diode.php (Accessed: 12 December 2023).
[52]. Rashid, G. and Ali, M.H. (2023) FRT capability enhancement of Offshore Wind Farm by DC Chopper, MDPI. Available at: https://www.mdpi.com/1996-1073/16/5/2129 (Accessed: 10 December 2023).
[53]. Selvy, P.T., Palanisamy, Dr.V. and Radhai, M.S. (no date) Image segemntation using cluatering technique ans swarm INTELLIANGE, Journal of Global Research in Computer Sciences. Available at: https://www.rroij.com/open-access/image-segemntation-using-cluatering-technique-ans-swarm-intelliange.php?aid=38372 (Accessed: 13 December 2023).

Appendices

Appendix A.

Implementation of a MPPT controller using Particle Swarm Optimization.

```
function DutyCycle = OptimizePSO(Voltage, Current)

% DutyCycle output = Value for the duty cycle of the boost converter (0 to 1)

% Voltage input = Terminal voltage of PV array (V)

% Current input = Current of PV array (A)

% Param inputs:
% InitialDuty = Param(1); % Starting value for DutyCycle
% MaxDuty = Param(2); % Upper limit for DutyCycle
% MinDuty = Param(3); % Lower limit for DutyCycle
% StepSize = Param(4); % Step size for adjusting DutyCycle
DutyCycle = 0.001; % Starting value for DutyCycle
MaxDuty = 0.59; % Upper limit for DutyCycle
MinDuty = 0; % Lower limit for DutyCycle
StepSize = 0.01; % Step size for adjusting DutyCycle
inertiaWeight = 0.9;

persistent CurrentDutyMatrix PrevPower Velocity CurrentMaxPower PrevMaxPower NewPower
BestGlobalDuty BestPersonalDuty NewDutyMatrix
VelocityRange = [-StepSize, StepSize];
Population = 100;

 % Inertia weight range
 LearningFactors = [1.2, 1.2];

if isempty(PrevPower)
```

```
    % Initialize matrices
    PrevPower = zeros(1, Population);
    NewPower = zeros(1, Population);
    Velocity = zeros(1, Population);
    NewDutyMatrix = zeros(1, Population);
    CurrentDutyMatrix = rand(1, Population);
    Velocity = rand(1, Population) * (VelocityRange(2) - VelocityRange(1)) + VelocityRange(1);

    % Enforce boundaries
    for i = 1 : Population
        CurrentDutyMatrix(i) = min(max(CurrentDutyMatrix(i), MinDuty), MaxDuty);
    end

    % Calculate initial power
    for i = 1:Population
        DutyCycle = CurrentDutyMatrix(i);
        PrevPower(i) = Voltage * Current;
    end
    [PrevMaxPower, globalIndex] = max(PrevPower);
    BestPersonalDuty = CurrentDutyMatrix;
    BestGlobalDuty = CurrentDutyMatrix(globalIndex);
end

iteration = 0; MaxIterations = 10;

while iteration < MaxIterations
    iteration = iteration + 1;
    % Power calculation
    for i = 1:Population
        DutyCycle = CurrentDutyMatrix(i);
        NewPower(i) = Voltage * Current;
```

```
    end

    % Update best duties
    for i = 1:Population
        if NewPower(i) > PrevPower(i)
            PrevPower(i) = NewPower(i);
            BestPersonalDuty(i) = CurrentDutyMatrix(i);
        end
    end

    % Update global best duty
    [CurrentMaxPower, index] = max(PrevPower);
    if CurrentMaxPower > PrevMaxPower
        PrevMaxPower = CurrentMaxPower;
        BestGlobalDuty = CurrentDutyMatrix(index);
    end

    inertiaWeight = 0.8;
    % Velocity matrix calculation
    for i = 1:Population
        Velocity(i) = (inertiaWeight * Velocity(i) + LearningFactors(1) * rand * (BestPersonalDuty(i) -
CurrentDutyMatrix(i)) + LearningFactors(2) * rand * (BestGlobalDuty - CurrentDutyMatrix(i)));
    end
  % Update positions
    NewDutyMatrix = CurrentDutyMatrix + Velocity;
    % Enforce limits
    NewDutyMatrix = min(max(NewDutyMatrix, MinDuty), MaxDuty);
    CurrentDutyMatrix = NewDutyMatrix;
end
[~, globalIndex] = max(NewPower);
DutyCycle = CurrentDutyMatrix(globalIndex);
end
```